Advanced Functional Materials

ADVANCED FUNCTIONAL MATERIALS
www.afm-journal.de

REVIEW OPEN ACCESS

From Clinic to Computation: Multiscale Bioengineering Strategies for Durable Biological Aortic Valve Replacements

Gabriele Greco[1,2] | Pierfrancesco Gaziano[3] | Serena Anglese[4] | Simone Morganti[1] | Carlo de Vincentiis[4] | Ferdinando Auricchio[1] | Michele Marino[3] | Michele Conti[1,4]

[1]Department of Civil Engineering and Architecture, University of Pavia, Pavia, Italy | [2]Department of Animal Biosciences, Swedish University of Agricultural Sciences, Uppsala, Sweden | [3]Multiscale and Multiphysics Mechanics Group (M2M), Department of Civil Engineering and Computer Science Engineering, University of Rome Tor Vergata, Roma, Italy | [4]3D and Computer Simulation Laboratory, IRCCS Policlinico San Donato, San Donato Milanese, Italy

Correspondence: Gabriele Greco (gabriele.greco@slu.se)

Received: 4 November 2025 | **Revised:** 11 February 2026 | **Accepted:** 11 February 2026

Keywords: constitutive modelling | heart valves | medical device | structural valve degradation | tissue mechanics

ABSTRACT

Bioprosthetic aortic valves, especially those implanted via transcatheter methods, have transformed the treatment of aortic stenosis. Nevertheless, their long-term durability is still limited by structural valve deterioration. While clinical and hemodynamic factors have been extensively reviewed, the material science perspective on bioprosthetic valve deterioration has received comparatively less attention. Structural valve deterioration is, however, a complex, multiscale, and multifactorial process, in which mechanical fatigue and calcification of bovine or porcine pericardial tissue play central roles.

For this reason, this review focuses on the pericardium itself—the engineered soft tissue at the core of bioprosthetic valves. The experimental techniques used to characterize its properties across multiple length scales, from molecular composition to macroscopic mechanics, are examined, highlighting how these multiscale measurements reveal critical structure–function relationships. Such insights are crucial for more accurate modeling of pericardial behavior and for understanding its deterioration in vivo.

By integrating bioengineering, advanced physical characterization, and computational modeling, a framework is outlined that links material properties to valve-level performance and, ultimately, clinical durability. This perspective not only advances the fundamental understanding of structural valve deterioration but also provides guidance for designing next-generation bioprosthetic and synthetic polymeric valves with improved longevity.

1 | Introduction

The aortic valve, located within the aortic root, ensures unidirectional blood flow from the left ventricle to the aorta through the coordinated motion of its three cusps and surrounding structures (Figure 1a) [1]. Native aortic valve leaflets are organized into three mechanically integrated layers: the fibrosa, spongiosa, and ventricularis [2, 3]. The fibrosa, located on the aortic side, is rich in densely aligned type I collagen fibers that provide tensile strength and resistance to diastolic pressure. The ventricularis, facing the left ventricle, is rich in elastin fibers arranged in a lamellar network, enabling rapid recoil and efficient leaflet opening during systole. Between these layers, the spongiosa facilitates shear deformation and dissipates mechanical stress. This highly organized collagen–elastin architecture is maintained by valvular interstitial cells, which regulate the extracellular matrix turnover and remodeling in response to mechanical cues [4].

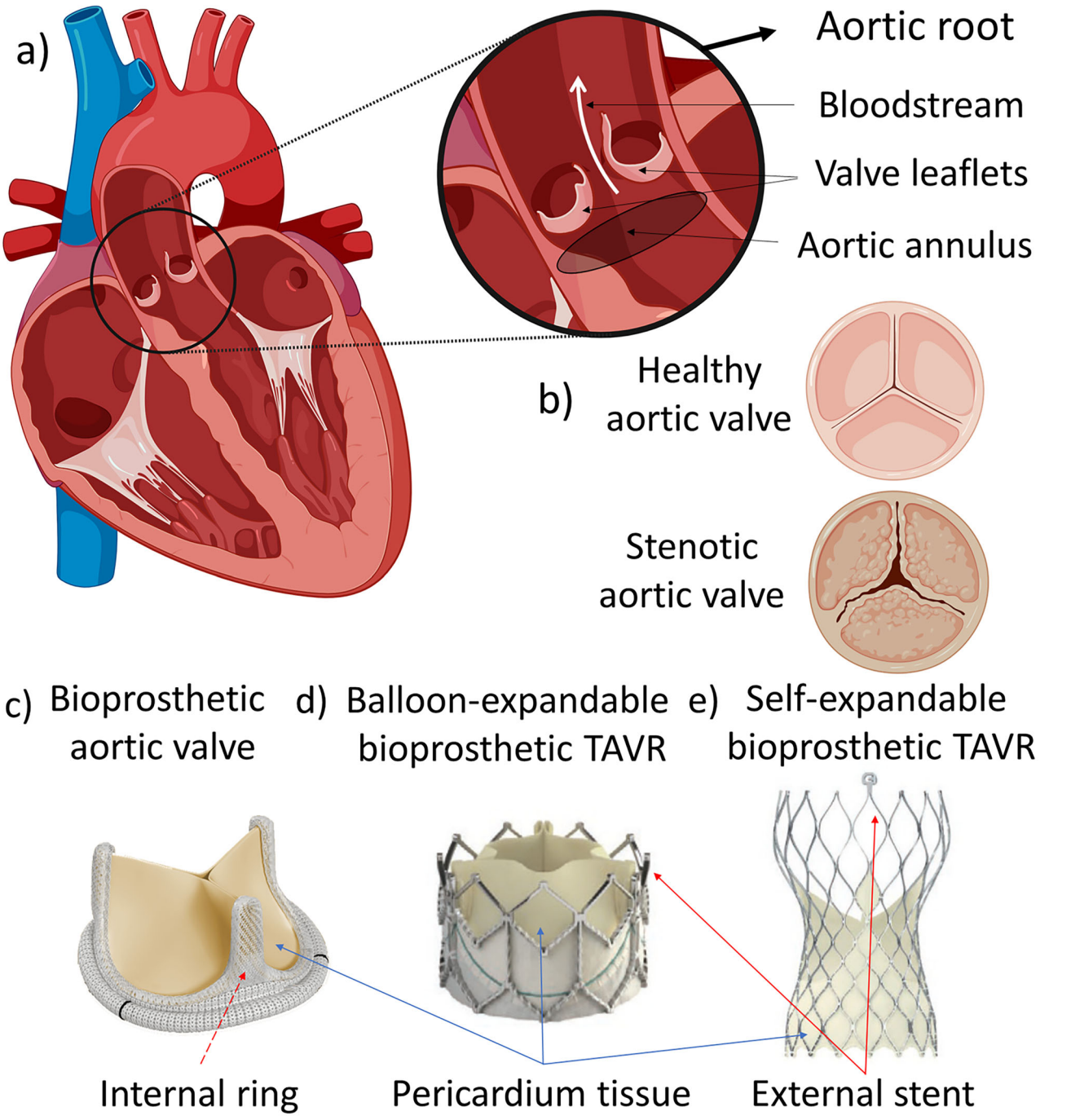

FIGURE 1 | (a) Schematic of the heart and the aortic root. Main anatomical features of the aortic valve. (b) Schematics of a healthy and stenotic aortic valve. General structure of biological prosthetic valves. (c) Bioprosthetic aortic valves that are usually implanted using open-heart surgery. Their structure is generally simpler with respect to (d) balloon-expandable and (e) self-expandable bioprosthetic aortic valves, generally implanted using transcatheter aortic valve replacement (adapted with permission from [5], Elsevier Inc 2021). This review will focus on (d) and (e). Created with Biorender.com.

Degradation of aortic valvular tissue can disrupt this delicate balance, leading to either aortic stenosis or aortic regurgitation, the two most common forms of aortic valve disease [6–8] (Figure 1b). Both conditions compromise cardiac performance, threatening the lives of numerous patients worldwide [9–11].

The diagnosis of such diseases relies on imaging modalities such as echocardiography, computed tomography, and magnetic resonance imaging to assess valve structure, function, and disease progression, guiding timely intervention [12]. Definitive treatment usually requires prosthetic valve replacement to prevent irreversible cardiac damage [13].

Prosthetic aortic valves can be either mechanical or biological [14–16]. Mechanical valves offer excellent durability but necessitate lifelong anticoagulation, increasing the risk of bleeding. Biological valves, in contrast, provide superior hemodynamics, lower thrombogenicity, and do not make noise, which are features

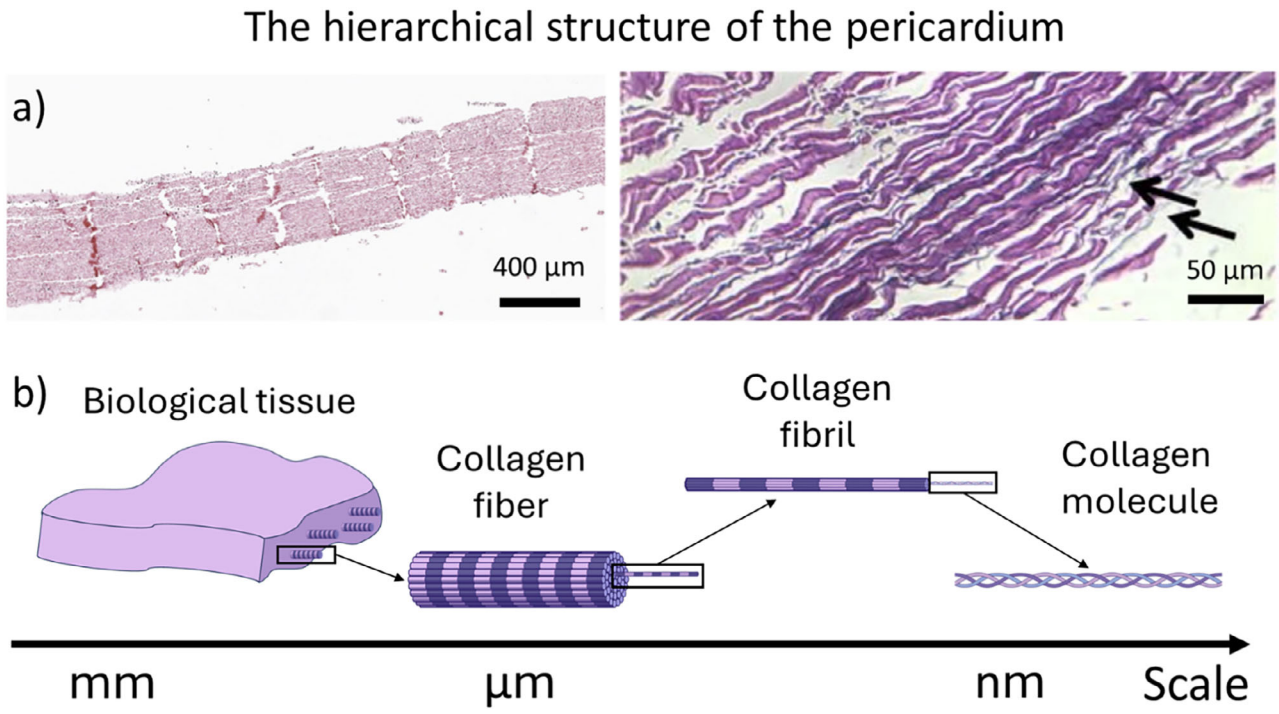

FIGURE 2 | (a) Histological sections of the pericardium tissue stained with H&E to highlight the fibrillar structure of the pericardium. The black arrows indicate the fibrils. Adapted with permission from [39] American College of Cardiology Foundation 2018. (b) Schematic of the hierarchical structure of collagen-based biological materials. Collagen fibrils and fibers interact in a complex network, whose physical properties depend on the types and quantities of inter-fibers/fibrils interactions. Created with Biorender.com.

often preferred by patients and frequently favored by clinicians, especially in elderly patients [13, 17–21].

Bioprosthetic valves exist in different types and can be implanted either surgically or through Transcatheter Aortic Valve Replacement—TAVR—(Figures 1c–e). This minimally invasive procedure has gained wide acceptance for its suitability for high-risk patients and potential benefits in small annuli [22–27]. Furthermore, it is associated with lower procedural costs compared to open-heart surgery [28].

TAVR devices are generally balloon-expandable, offering high radial force and precise placement, or self-expandable, which adapt more easily to complex anatomies (Figures 1d,e) [5]. Device selection depends on both anatomical features and patient-specific conditions [29–32].

Biological valves can consist of a fabric-covered stent onto which chemically treated porcine or bovine pericardium is mounted [33, 34]. Pericardial tissue exhibits a hierarchical structure (Figures 2a,b): collagen fibers and fibrils, which are often arranged helically and with varying degrees of alignment, are embedded in an extracellular matrix where interactions are mediated by proteoglycans and other molecules [35–37]. These microstructural features play a crucial role in determining the tissue's mechanical properties, including its anisotropic nature and resistance to fatigue [38].

To reduce immunogenicity and improve durability, pericardial tissue for bioprosthetic heart valves is commonly decellularized and then cross-linked with glutaraldehyde: typically at concentrations below 1.5% for variable durations [40]. The specific processing parameters have a strong influence on the mechanical and biological properties of the tissue. Glutaraldehyde treatment stabilizes the material, enhancing its strength and stiffness; however, residual aldehyde groups may react with surrounding tissues, potentially initiating long-term degradation processes [41].

Porcine bioprosthetic valves can also be derived from native pig aortic valves treated with glutaraldehyde to reduce immunogenicity [42]. In contrast to porcine pericardial valves, native pig aortic valve leaflets are directly mounted on a supporting stent, retaining their natural geometry and exhibiting physiological opening and closing dynamics, though production is difficult to standardize due to anatomical variability among animals [43].

The performance of a bioprosthetic valve is fundamentally determined by the properties of the tissue from which it is made. As such, any structural degradation of this tissue leads to impaired mechanical function and, eventually, valve failure. Among the causes of long-term failure, Structural Valve Deterioration (SVD)—defined as permanent intrinsic changes to the valve biological tissue or frame that lead to clinically relevant valve dysfunctions—remains the major limiting factor in the durability of TAVR prostheses [44], and it represents the central focus of this review. Given the multifactorial nature of SVD, spanning biological, mechanical, and clinical dimensions, a comprehensive evaluation requires integrating knowledge across these domains. To address this challenge, we aim to compile and critically evaluate current knowledge on structural valve degradation through a multidisciplinary lens.

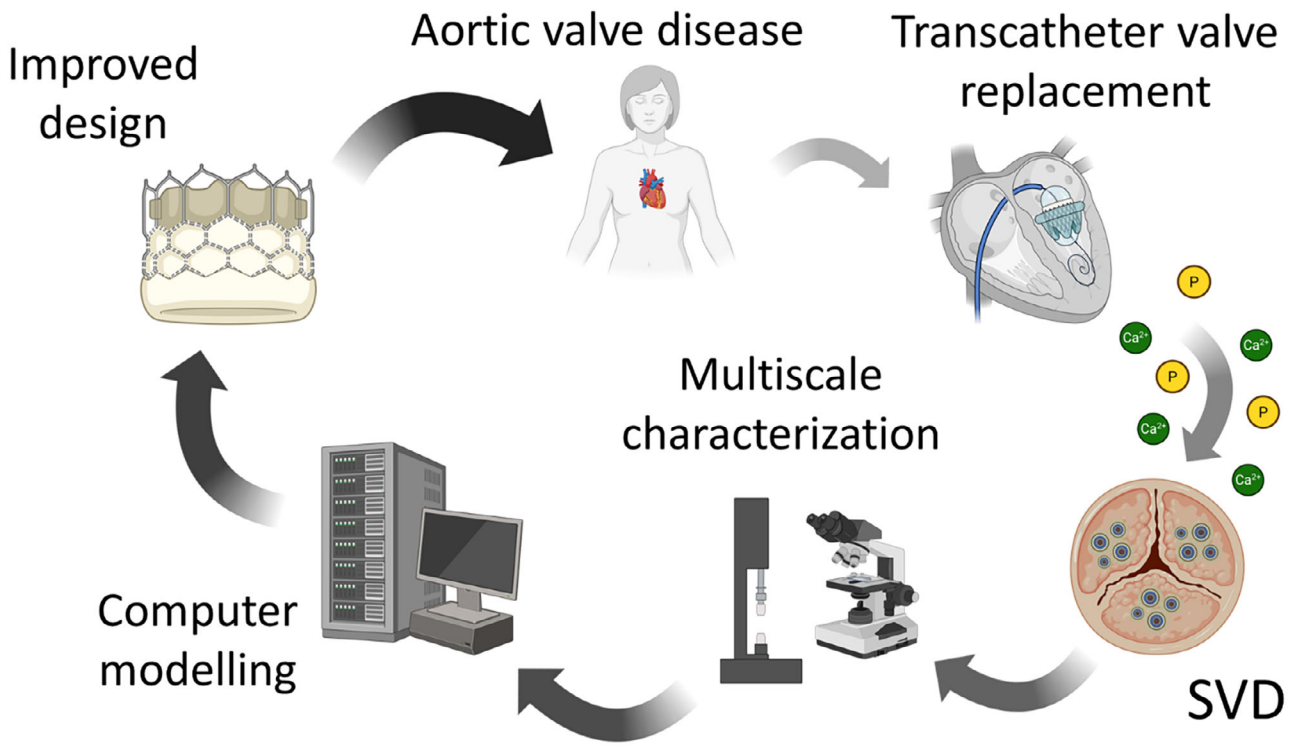

FIGURE 3 | Schematic of the review and the path toward more durable bioprosthetic aortic valves. After the implantation, the bioprosthetic valve ceases to work due to Structural Valve Deterioration (SVD), in a range spanning 5–10 years [45]. To understand this phenomenon and prevent it, a multiscale physical characterization is required. With accurate experimental physical data, we can inform computational models and enhance the design of bioprosthetic and polymeric aortic valves. Created with Biorender.com.

Figure 3 presents the conceptual framework of the review. Preventing SVD requires a deep understanding of its underlying mechanisms, which are inherently multiscale and multifactorial. Given that bioprosthetic valves are composed of biological materials, their degradation is tightly linked to how these tissues respond to mechanical loading, fatigue, and biochemical stimuli.

To this end, we emphasize the need for experimental characterization across multiple scales — from the nano and microstructure of extracellular matrix proteins to the macroscopic mechanical and hemodynamic performance of the valve. Establishing these structure–function relationships in pericardial tissue is crucial for developing accurate computational models. Such models, in turn, provide predictive capabilities to simulate degeneration scenarios and support the design of next-generation prostheses with improved resistance to SVD.

Although this review focuses on bioprosthetic aortic valves, many of the challenges and insights discussed here are broadly applicable to other valve types [46]. For instance, findings presented for aortic valves can often be extended to mitral valve replacements, provided that differences in operating conditions (e.g., higher pressures and distinct geometries) are taken into account [47].

Finally, while the primary focus of this work is on bioprosthetic devices, we also briefly address polymeric heart valves. Although the failure and degradation mechanisms of bioprosthetic valves differ substantially from those of synthetic polymeric valves, these emerging technologies share several mechanical and durability challenges. In this context, cross-disciplinary knowledge exchange may help accelerate innovation and ultimately improve clinical outcomes.

2 | Structural Valve Deterioration—A Clinical Perspective

Over time, bioprosthetic aortic valves may progressively lose their functionality, leading to clinical complications and, eventually, reintervention. The onset and rate of failure depend on both the type of prosthesis and patient-specific factors [45, 48]. The main mechanism responsible for this degeneration is Structural Valve Deterioration (SVD)—a process of morphological and hemodynamic alteration that limits the long-term durability of bioprosthetic valves.

The definition of SVD has evolved from descriptive terminology to standardized, hemodynamic-based classifications [49–52]. According to the European consensus [53], SVD progresses through stages characterized by increasing structural and functional impairment:

- Stage 0–1: Morphological leaflet abnormalities (thickening, calcification, motion disorder) without significant hemodynamic impact.
- Stage 2S/2R/2RS: Moderate stenosis and/or regurgitation, defined by transvalvular gradient increase (>10 mmHg) or regurgitant flow quantification.

- Stage 3: Severe stenosis and/or regurgitation requiring clinical intervention.

Interestingly, while this staging bears conceptual similarities to the grading of native aortic stenosis, which is also classified as mild, moderate, or severe based on hemodynamic parameters, there are important distinctions [54, 55]. Native stenosis reflects progressive disease of the patient's own valve, whereas SVD arises from degeneration of a bioprosthetic device. SVD staging combines structural imaging (leaflet changes) with functional impact (gradients, regurgitation), whereas native stenosis grading relies primarily on hemodynamic severity. In SVD, the presence of regurgitation is particularly emphasized as part of the staging, reflecting prosthesis-specific failure modes, while in native stenosis, regurgitation is considered separately. Finally, the gradient thresholds differ because prosthetic valves typically exhibit higher baseline transvalvular gradients than native valves of equivalent orifice area.

The staging strategy used to classify SVD allows systematic monitoring of valve performance, although the progression timeline is patient-dependent. For example, Stage 2S patients are typically followed every 3–6 months, while annual check-ups are recommended post-implantation for all cases [56].

Echocardiography remains the gold standard for diagnosis and follow-up, using transthoracic or, when needed, transesophageal imaging [57, 58]. Doppler measurements provide a quantitative assessment of gradients and flow, though interpretation can vary with valve size, type, and anatomy [59]. Early SVD stages are often hemodynamically silent and defined primarily by morphological signs.

Complementary modalities such as multidetector computed tomography (MCT) offer high-resolution insights into leaflet morphology, thrombosis, and calcification [60, 61]. MCT is particularly valuable for quantifying calcium burden and for supporting biomechanical model validation, as it provides data on leaflet deformation and stiffness. Although its routine clinical use is still limited by accessibility and expertise, adoption is increasing worldwide [62]. Magnetic resonance imaging (MRI) and ultrafast pulse wave velocity measurements are emerging as adjunct tools, capable of detecting SVD-related functional changes and vascular stiffness [63].

Despite these advances, current clinical imaging and staging systems describe what happens during SVD, but not why it occurs. They provide a limited understanding of the physical and biological mechanisms driving tissue degeneration. To move from observation to prevention, it is necessary to complement clinical data with insights into the material, structural, and mechanical origins of valve failure.

This transition—from descriptive clinical evaluation to mechanistic comprehension—defines the next step toward innovation. The following sections, therefore, adopt a bioengineering perspective, exploring how experimental testing, multiscale characterization, and computational modeling can elucidate the mechanisms of SVD and guide the development of more durable, next-generation bioprosthetic valves.

3 | Structural Valve Deterioration—A Bioengineering Perspective

Aortic valve deterioration involves a combination of biological and mechanical processes that progressively impair its function. In particular, bioprosthetic valves — especially those made from pericardial tissue — develop structural heterogeneities that reduce their capacity to deform and distribute stress evenly, ultimately affecting performance and long-term durability [64].

These heterogeneities in pericardial tissue may result from progressive thickening, inclusion of calcific deposits, irreversible plastic deformation of the protein network, and thrombus formation (Figure 4a). Among these processes, calcification and fatigue-induced damage represent the most critical drivers of long-term degeneration and will be the focus of this section.

3.1 | Calcification

Tissue mineralization, commonly referred to as calcification, is a leading cause of SVD [65–67]. Although the precise mechanisms underlying calcification remain incompletely understood, it is widely believed to originate from interactions between circulating calcium ions in the blood and valve tissue that has been either mechanically damaged or chemically altered by glutaraldehyde fixation. Notably, native (non-crosslinked) tissues exhibit lower susceptibility to mineralization [68], as they retain natural mechanisms to inhibit calcium phosphate nucleation. In contrast, glutaraldehyde-fixed tissues lose this capacity, allowing calcium (from the blood) and phosphate (from damaged membranes) to coalesce and form crystals within the valve matrix [69]. As these crystals nucleate and grow, they deform the valve structure, ultimately compromising function and leading to failure [70, 71]. For instance, calcification on valve cusps impairs leaflet mobility, leading to aortic stenosis [72, 73]. Furthermore, recent findings indicate that valve calcification is characterized by the presence of two distinct mineral populations: calcified collagen fibers with dimensions ranging from 0.5 to 6.4 μm, and calcium phosphate particles of approximately 1 μm in size, originating from host cellular activity [74]. The same study also demonstrated a reduction in collagen fibril diameter in regions adjacent to calcified deposits, highlighting how calcification is accompanied by progressive tissue damage and microstructural remodeling.

When discussing calcification, it is also important to consider that calcium deposits may differ in their physicochemical nature, comprising amorphous calcium phosphate rather than crystalline hydroxyapatite, as recently demonstrated for native aortic valve leaflets by Sivaguru and co-authors [75].

Table 1 summarizes recent data on pericardial tissue calcification, highlighting trends in calcium accumulation over time. A clear finding is that the method of crosslinking has a substantial effect on mineralization behavior. However, most in vitro studies cover only short timeframes (typically less than three months), whereas clinical valve failure may take years to manifest. Moreover, wide variability in calcium deposition is observed even among studies using comparable protocols [76, 77]. This inconsistency highlights the need for standardized methods and longer-term studies to

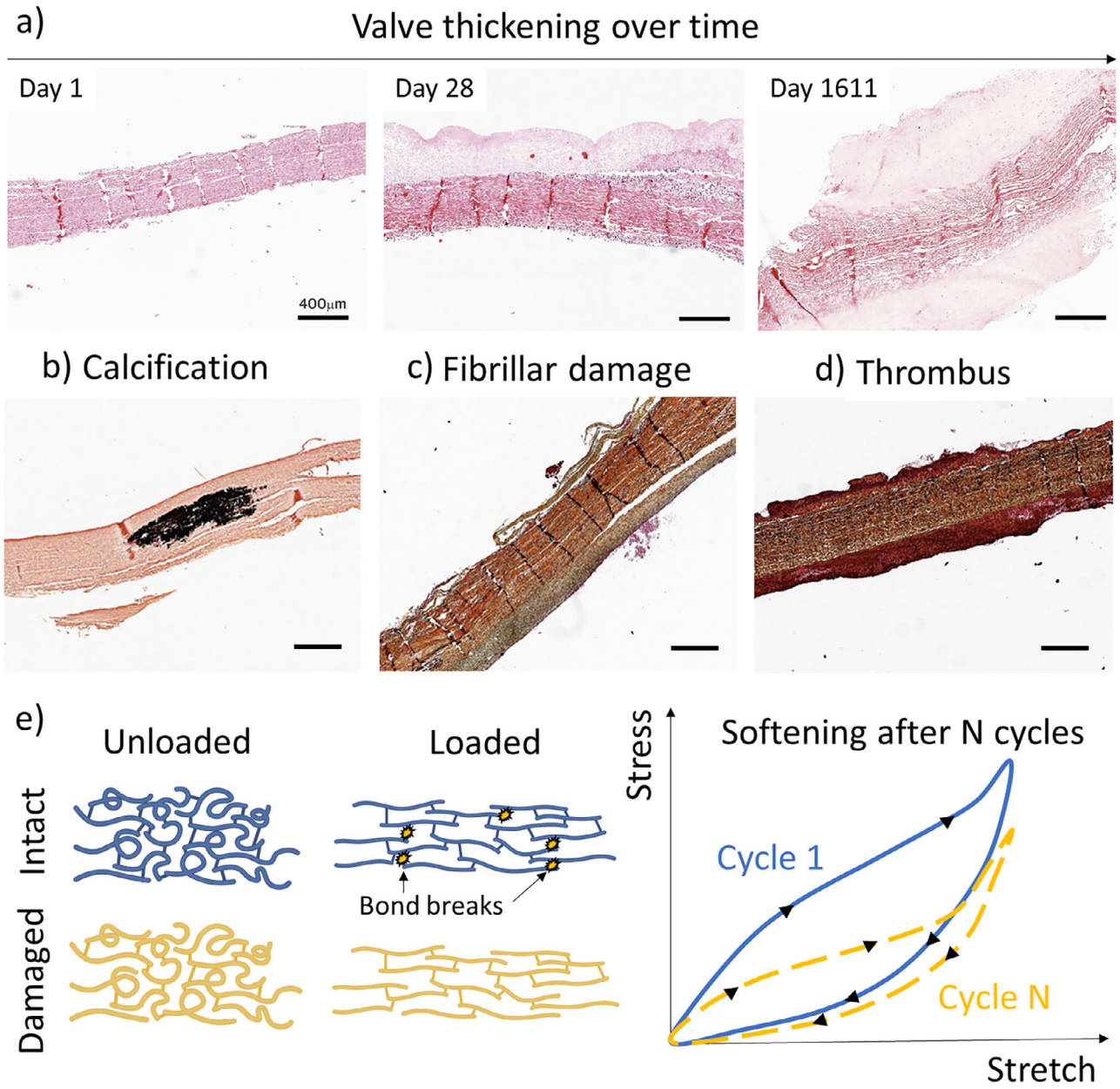

FIGURE 4 | Examples of histological sections of degraded bioprosthetic aortic valves, adapted with permission from [39], American College of Cardiology Foundation, 2018. (a) Over time, the valves show noticeable thickening. We show the effect of (b) calcification that leads to the formation of nucleated crystals. Additionally, (c) fibril damage caused by fatigue can impair the mechanical performance of the valve and promote (d) thrombus formation. (e) Schematic of the stress softening (Mullins effect) in a protein-based network under cyclic loading. Once damage occurs, the network becomes less able to sustain loads, resulting in a softer response. Created with BioRender.

evaluate how crosslinking chemistry affects calcification kinetics in bioprosthetic materials [74].

To mitigate glutaraldehyde-related calcification, several strategies have been proposed [86, 87]. Many approaches include both systemic interventions (e.g., statins) and local modifications such as advanced crosslinking chemistries and surface coatings [76, 85, 85]. For example, Yu et al. developed a new porcine pericardium crosslinked with octafunctionalized polyhedral oligomeric silsesquioxane-terminated polyethylene glycol via Schiff base reactions [77]. This method reduced calcification by a factor of 80 compared to glutaraldehyde. Pu et al. used atom transfer radical polymerization to graft a double-bonded monomer onto bromide-functionalized pericardium, achieving a 50-fold reduction in calcium deposition [79]. Additionally, Zhang et al. applied decellularization protocols with Triton X-100, sodium dodecyl sulfate, and sodium deoxycholate, reporting a two-fold reduction in calcium after 21 days and up to eight-fold after 60 days, compared to glutaraldehyde-fixed tissue [63]. Lastly, Shi et al. combined oxidized chondroitin sulfate crosslinking with copper-doped carbon dots, achieving promising results in structural stability and mineralization inhibition [81].

Other strategies to reduce calcification focus on neutralizing glutaraldehyde residues. For instance, post-treatment with sodium

TABLE 1 | Main recent results regarding the amount of calcified tissue measured in vitro vs the type of treatment used to cross-link the pericardium tissue.

Refs.	Per. type	Treatment	Ca 15 days (μg/mg)	Ca 21 days (μg/mg)	Ca 30 days (μg/mg)	Ca 60 days (μg/mg)	Ca 90 days (μg/mg)
[78]	Bovine	None	0.2		0.46	0.96	
	Bovine	glutaraldehyde (NA)	29.8		50.72	127.49	
	Bovine	eHTCC	1.51		1.71	1.06	
[77]	Porcine	glutaraldehyde (0.625%, 37°C, for 1 day)			125	175	225
	Porcine	POSS-PEG-CHO			2	2.5	2.5
[79]	Porcine	glutaraldehyde (0.625%, NA)			75.24	155.16	
	Porcine	PT			2.88	4.92	
	Porcine	PT-BS			2.91	4.29	
[80]	Bovine	glutaraldehyde (1%, NA, 2 days)				200	
	Bovine	M2-EXO-BP				57	
[81]	Bovine	glutaraldehyde (0.625%, 37°C, for 3 days)			82		300
	Bovine	OCS			50		40
	Bovine	Cu-CDs-OCS			15		10
[82]	Bovine	glutaraldehyde (0.625%, NA)		4		9	
	Bovine	TX-DNG		1.8		0.9	
	Bovine	SDC-DNG		1.6		1	
	Bovine	SDS-DNG		2		0.9	
[83]	Porcine	None	2		2.3		
	Porcine	glutaraldehyde (0.625%, RT, 2 days)	4.4		5.7		
	Porcine	STS	0.5		1.2		
[84]	Porcine	glutaraldehyde (0.625%, NA, 7 days)			48		221
	Porcine	Zr			4		25
	Porcine	PGSB/Zr			3		6
[85]	Porcine	None	2		2.3		
	Porcine	glutaraldehyde (0.625%, NA)	4.5		6		
	Porcine	CHPP	0.4		1.5		
[76]	Bovine	None	1		1.5		
	Bovine	glutaraldehyde (0.625%, 37°C, 1 day)	1.7		2.5		
	Bovine	Glyoxal and Glutamic Acid	1.2		1.9		

NA = information Non Available; RT = Room Temperature.

thiosulfate has been shown to reduce calcification by more than 75% [83].

In vitro calcification tests are widely used to assess the calcification propensity of bioprosthetic valve materials. Traditional static immersion methods often suffer from low reproducibility, whereas dynamic systems better mimic physiological loading and flow [88]. Reproducible in vitro tests provide a cost- and time-efficient means to benchmark materials and optimize anti-calcification strategies, representing an important step toward harmonized preclinical evaluation. In this context, Kiesendahl and colleagues developed a standardized dynamic test using a near-physiological, non-spontaneously precipitating fluid, enabling reliable discrimination of calcification tendencies between materials [89], and their approach was further validated in a subsequent comparative study [90]. While calcification is one of the primary mechanisms of valve degeneration, it often coexists with and is exacerbated by fatigue-induced damage of the tissue, as discussed below.

3.2 | Fatigue Damage and Plastic Deformation

Native heart valves are exposed to over 3 billion cycles of opening and closing during a person's lifetime and are remarkably resistant to fatigue. In contrast, bioprosthetic valves experience progressive mechanical deterioration under cyclic loading. A key manifestation of this is stress softening (also known as the Mullins effect), whereby tissue stress diminishes over repeated load cycles (Figure 4e) [91].

At the molecular level, fatigue in pericardial tissue stems from the progressive rearrangement and eventual failure of interactions between collagen fibrils and their inter-linkers, e.g., proteoglycans [35]. As cyclic loading stretches the collagen network, fibrils slide and reorient, leading to permanent deformations and weakened load-bearing capacity [92]. This deterioration begins as early as the first cycle and manifests as a lower unloading stress compared to the loading stress at the same strain [93]. As these interactions degrade, the material becomes progressively plasticized, accumulating residual strain and ultimately failing.

It is widely accepted that the tissue's resistance to progressive damage and fatigue depends on the density and quality of intermolecular interactions in its protein network [94–97]. Consequently, fatigue behavior can vary significantly depending on the animal source and fixation method. For example, glutaraldehyde-fixed bovine pericardium exhibits greater fatigue resistance than native bovine or porcine pericardium, likely due to an enhanced crosslinking density [98]. To the best of our knowledge, all commercially available bioprosthetic heart valves are manufactured using glutaraldehyde-based fixation methods [99]. This is largely because, despite its well-known drawbacks (e.g., calcification), glutaraldehyde fixation provides reliable tissue stabilization, effective antigen masking, and acceptable hemocompatibility [100]. For this reason, identifying alternative treatments that can simultaneously match the mechanical performance, long-term durability, and biological behavior of glutaraldehyde-fixed tissues remains highly challenging. In addition, market inertia likely plays a role, as glutaraldehyde-fixed valves have represented the clinical standard for decades, and existing manufacturing processes are strongly optimized around this technology. Nonetheless, we discuss below some of the most recent trends in alternative fixation strategies.

Improving the pericardial tissue's resistance to fatigue hinges on reinforcing its protein architecture. One promising method, developed by Li et al., involves sequential zwitterionic surface modification and zirconium-based crosslinking of porcine pericardium [84]. This approach maintained low transvalvular pressure gradients even after 200 million fatigue cycles.

A complementary strategy involves forming a secondary polymer network within the collagen matrix, inspired by the design of synthetic materials. For example, Wang et al. created a toughened fully synthetic elastomer by embedding a stiff, self-assembling polymer into a primary polymer network, resulting in a fivefold increase in fatigue resistance [101]. Such dual-network strategies aim to enhance the material's topological entanglements, a concept that is also being successfully applied in protein-based materials [102]. These principles could similarly be exploited to enhance the longevity of bioprosthetic valves.

Another frontier for improving fatigue resistance of bioprosthetic valves lies in self-healing materials. If the collagen network could restore its broken bonds during loading cycles, fatigue resistance would be dramatically improved [103]. Natural pericardium already possesses a limited self-healing capacity via hydrogen bonds between proteoglycans and collagen. These features have inspired bioinspired polymeric self-healing systems [104, 105]. Additionally, the high mobility of collagen fibrils, which allows reorientation under load, is known to enhance toughness and fatigue resistance [38]. Therefore, enhancing hydrogen bonding and network mobility should, in principle, improve fatigue performance.

Though native pericardium is more complex than synthetic systems, Jastrzebska and colleagues demonstrated that glutaraldehyde fixation increases hydration, but localizes water between fibrils rather than within them [106–108]. This increased fibrillar spacing may weaken hydrogen bonds and reduce fatigue performance. They proposed tannic acid treatment as a solution, since it can form extensive hydrogen bonds with proteins. Indeed, tannic acid-treated porcine pericardium showed improved structural stability, although fatigue testing has yet to be conducted.

3.3 | Coupling Between Mechanical Fatigue Damage and Calcification

Long-term degeneration of bioprosthetic heart valves arises from a coupled interaction between fatigue-related microstructural evolution under cyclic loading and progressive calcification, rather than from independent or additive mechanisms. Cyclic loading induces fibre recruitment, unfolding, and Mullins-type softening, which locally weakens the collagen network and alters stress distributions, while calcification introduces localized stiffening that further amplifies mechanical heterogeneity. Experimental evidence indicates that fatigue damage can promote calcification by creating preferential calcium binding sites within disrupted collagen fibres, leading to spatially heterogeneous mineral accumulation [109]. Complementarily, accelerated durability testing in calcifying environments shows that mineral deposition preferentially occurs in regions subjected to elevated mechanical stresses, such as commissures and leaflet nadirs, and can significantly affect valve hydrodynamic performance [110]. These observations highlight a mechanobiological feedback between fatigue and calcification and suggest that their relative contributions to failure cannot be robustly quantified in isolation, underscoring the need for integrated experimental and computational frameworks to assess their combined role in long-term valve durability.

Understanding the interplay between calcification and fatigue is essential to unraveling the long-term durability of bioprosthetic valves. This, in turn, requires a deeper exploration of the physical and biochemical properties of pericardial tissue, which starts with rigorous experimental characterization.

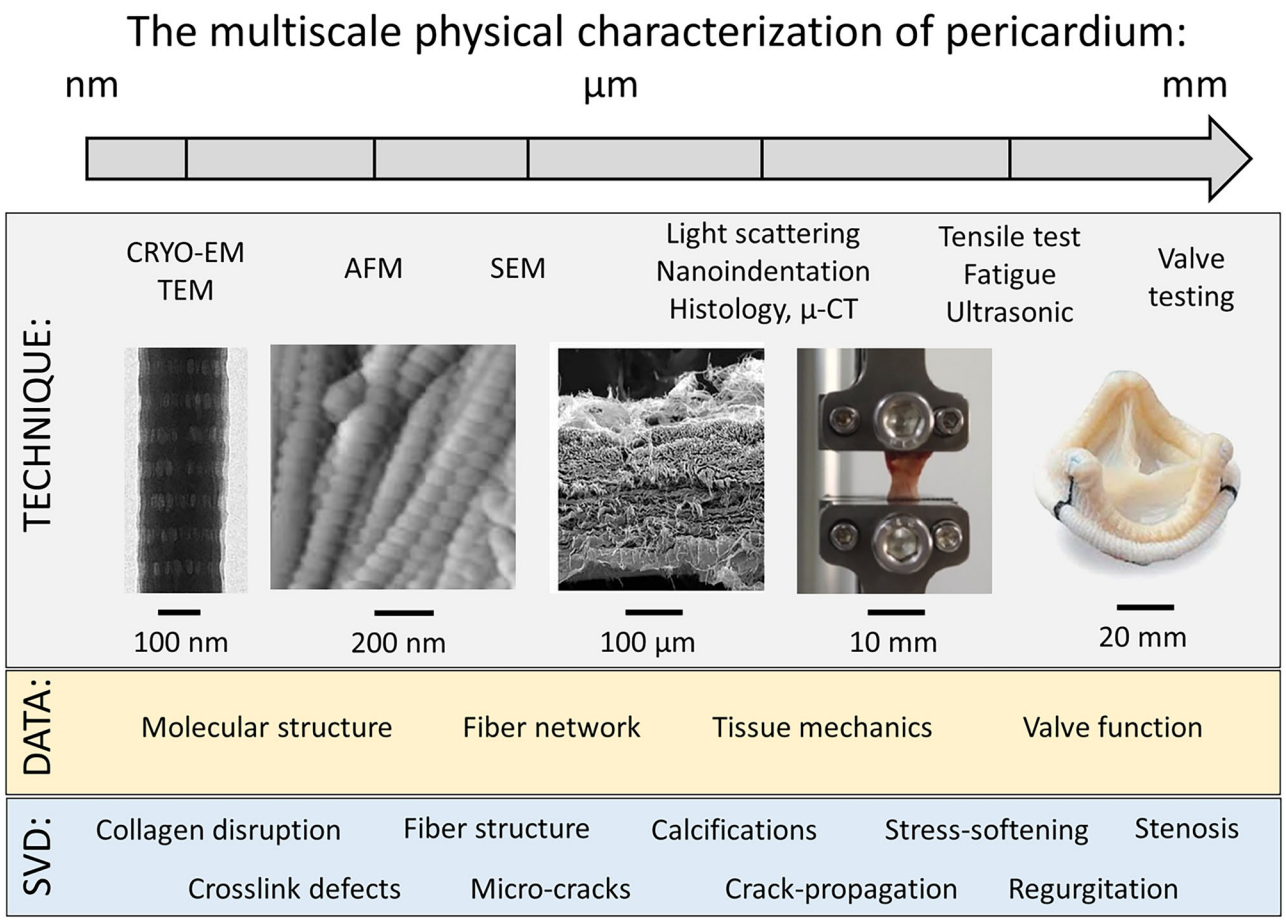

FIGURE 5 | The multiscale physical characterization of the pericardium. This image illustrates the main physical techniques used to characterize pericardial tissue, along with the scale at which they operate. For each technique and scale, the key data obtained are presented, along with the typical information relevant to structural valve degradation. Image created from the adaptation, with permission, from [112–114]. Cardiovascular Research Foundation, 2021; Elsevier, 2021; Wiley, 2014. This figure was also created by using the raw data of [115, 116].

4 | Multiscale Physical Characterization of the Pericardium

SVD manifests across multiple dimensional scales. At the microstructural level, degraded pericardial tissue often exhibits protein network defects, microcracks, calcifications, and collagen fiber degeneration. These alterations compromise leaflet mechanics, ultimately leading to valve dysfunctions such as stenosis or regurgitation. Therefore, elucidating the mechanisms underlying SVD requires rigorous experimental and physical characterization of pericardial tissue.

Given that the macroscopic mechanical behavior of the tissue is fundamentally governed by the micro- and nano-scale structure of the protein network (particularly collagen) and the complex interactions among its constituent proteins, adopting a multiscale investigative approach is imperative.

Today, a variety of advanced techniques exist that enable the pericardium characterization across multiple scales, ranging from the nanometric organization of individual collagen molecules to the overall macroscopic fatigue response of the pericardium (Figure 5). Each technique operates at a specific dimensional scale and provides data that can be directly linked to structural valve deterioration. Despite their relevance, the diversity of these experimental approaches—and their potential to advance the development of more durable bioprosthetic valves—has been only rarely addressed in the literature [74, 111].

This section provides a comprehensive overview of these techniques, emphasizing the key challenges associated with their application and discussing potential strategies to address them. For clarity, we first examine the techniques used to investigate the structure and morphology of pericardial tissue. We then discuss the methods employed to determine its mechanical properties and fatigue behavior, including assessments of valve flow performance.

4.1 | Biochemical and Structural Composition of the Pericardium

The macroscopic mechanical behavior of structured materials is fundamentally governed by their internal micro- and nanostructure [117, 118]. This principle is especially pertinent to protein-based materials, where the architecture of the protein network plays a decisive role. To investigate this network, a range of analytical techniques can be employed. These techniques include

Fourier transform infrared spectroscopy, x-ray diffraction, and Raman spectroscopy.

The first critical step in analyzing the structure of pericardial membranes is verifying the integrity of the collagen matrix, even after cross-linking treatments have been applied. Specifically, it must be confirmed that collagen fibrils have not undergone degradation [119, 120]. Once this baseline is established, attention can shift to detecting structural features introduced by novel cross-linking strategies, such as interactions between specific amino acid residues [84]. For instance, the FTIR absorption peak at 1744 cm^{-1} is characteristic of H—C═O groups from glutaraldehyde cross-linking. Kong et al. exploited this peak to monitor the efficacy of residual glutaraldehyde removal through sodium thiosulfate treatment, aiming to reduce the calcification tendency of the treated pericardium [83].

However, it is important to recognize the limitations and potential artifacts associated with Fourier Transform Infrared (FTIR) spectroscopy. Jafari et al. demonstrated that in ATR-FTIR (Attenuated Total Reflection Fourier Transform Infrared) measurements, the contact pressure from the crystal prism can locally deform biological samples, thereby compromising the accuracy of the spectral data [121].

Another important caveat relates to the detectability of specific protein interactions. Topological interactions among protein or polymer chains (e.g., entanglements) are generally invisible to conventional spectroscopy techniques [122]. Yet these interactions may be central to enhancing bioprosthetic valve performance, particularly in improving fatigue resistance. Indeed, recent work on protein-based materials suggests that tuning topological interactions may serve as a valuable strategy for enhancing mechanical resilience [101, 102].

Beyond collagen, other matrix components also contribute to the mechanics of pericardial tissue. These non-collagenous elements are especially relevant during stress relaxation and unloading phases, where viscoelastic behavior is dominant [123].

In addition to analyzing specific molecular interactions, it is also essential to investigate the mesoscale organization of the collagen fiber network. Scattering light microscopy and birefringence experiments are particularly suitable for this purpose, as they enable nondestructive assessment of fiber alignment across tissue layers [98, 124]. However, care must be taken in interpreting results, as collagen fiber orientation can vary significantly across different pericardial layers [112, 125].

In general, a higher degree of collagen fiber alignment enhances the fatigue resistance of the tissue, particularly when loads are applied along the preferred fiber direction [126]. This makes it critical to consider the laminar architecture of the pericardium, as differential alignment across layers can lead to complex, nonuniform stress distributions under mechanical deformation [64]. An added advantage of light-scattering techniques is their compatibility with in situ mechanical testing. When combined, these methods enable real-time monitoring of collagen fiber orientation during deformation, a key factor underlying the exceptional toughness of collagenous tissues [38].

Once the micro- and nanostructure of the pericardium has been characterized, a deeper understanding of material degradation also requires examining the tissue's morphology and configuration across the nano- to microscale [74].

4.2 | Morphology and Micro and Nano Structural Characterization

Understanding the morphology and microstructure of biological samples requires a wide range of imaging techniques, chosen according to the dimensional scale of interest. For ultrastructural analysis, electron microscopy (EM) and its various modalities are indispensable. Among them, cryogenic electron microscopy (Cryo-EM) is one of the most powerful tools for resolving the molecular structure of biological materials [116]. Cryo-EM allows the identification of structural features such as collagen molecule alignment and the degree of molecular overlap, which can be visualized through grayscale banding patterns along fibrils [127]. These patterns can reveal the presence of nanoscale defects within collagen-based tissues.

At a larger dimensional scale, traditional Scanning Electron Microscopy (SEM) remains a fundamental tool for assessing the microscopic morphology of pericardial tissues and other cardiovascular structures [112]. However, EM techniques require extensive sample preparation, including dehydration, cutting, and downsizing [128]. These procedures can introduce artifacts that may alter the natural structure of the tissue. To mitigate this, alternative imaging methods are often necessary.

Among such alternatives, micro-computed tomography (micro-CT) can be employed to visualize the overall architecture and 3D morphology of pericardial samples in a nondestructive manner. CT-based techniques can also identify specific features, such as localized calcifications, which can then be integrated into finite element meshes to enhance the spatial resolution and realism of numerical simulations [129] (see section "Computational modeling of SVD"). This is especially relevant for models incorporating regional stiffness variations due to pathological changes.

As with many complex materials, a combined, multiscale imaging approach often yields the most complete understanding. For example, observing the waviness of collagen bundles on the fibrosa side of the aortic valve with SEM, and then co-registering that data with micro-CT scans, allows researchers to correlate structural patterns with mechanical responses under different loading conditions. Hasan et al. demonstrated that these wavy patterns flatten during diastole and reappear during systole, providing insight that can inform the optimization of bioprosthetic valve design [4].

Another important morphological feature is surface roughness, which significantly influences local blood flow turbulence and may promote tissue degradation and valve failure [130]. Surface roughness generally refers to the micrometric deviations of a surface's profile height from its mean line and can be quantified using various models. The simplest approach is to calculate the arithmetic average of these height deviations relative to the mean line. In this context, Atomic Force Microscopy (AFM) offers one

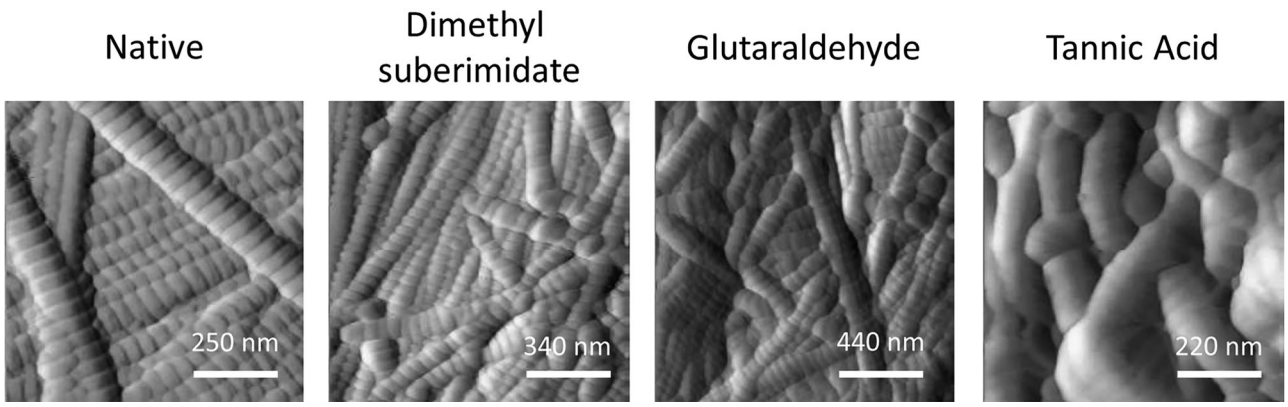

FIGURE 6 | Morphology of porcine pericardium treated with different cross-linking strategies investigated by means of AFM. The raw data to produce this figure were taken from [115] and processed with Gwyddion (64bit) [131].

of the most sophisticated tools for surface characterization at the nanometer scale and should be systematically applied across different classes of bioprosthetic valve tissues. For instance, Yu et al. analyzed porcine pericardium treated with various crosslinking agents using AFM [77]. Their results showed that crosslinking significantly reduced the spacing between collagen fibrils on the surface, resulting in a stiffer membrane response upon applied strain. Representative examples of chemically treated porcine pericardium surfaces are shown in Figure 6, clearly illustrating how different treatments drastically modify surface morphology and thus roughness.

It is generally accepted that the chemical or physical crosslinking of pericardial tissue results in denser fibrillar networks compared to untreated tissues [124]. This increase in fibrillar density is believed to enhance intermolecular interactions, thereby improving the mechanical performance of the membrane. Moreover, surface roughness is also a sensitive indicator of the material's degradation state. Studies have shown that higher roughness values are associated with collagen fibril damage [132], and rougher surfaces may increase exposure to the bloodstream, accelerating calcification processes [133].

Due to this exposure, it is also crucial to consider how the blood itself interacts with the bioprosthetic surface. In a recent study on healthy valves, Yin et al. demonstrated that the shear-thinning behavior of blood produces different shear stress conditions depending on surface roughness [134]. These altered stress fields may contribute to surface damage and deterioration, highlighting the importance of mechanical compatibility between blood rheology and valve surface properties.

Furthermore, surface roughness directly influences wettability, which is widely recognized as an important factor in blood–material interactions; however, the precise mechanisms by which hydrophilic or hydrophobic surfaces affect blood compatibility remain an active area of research with some contradictory findings in the literature. Chemically crosslinked membranes with higher wettability (i.e., lower contact angle) have been reported to perform better both mechanically and biologically [77, 81, 84]. Additionally, hydrophilic surfaces have been reported to be less prone to protein adsorption, a major contributor to thrombogenicity [135–137]. Therefore, optimizing surface properties to achieve hydrophilic behavior can help reduce the risk of thrombosis and extend the functional lifespan of the valve. However, wettability and protein interactions are interrelated in complex ways, and while hydrophilic surfaces are often associated with reduced thrombogenic responses, this association is not universally observed and appears to depend on additional surface chemical and physical characteristics as well as the biological environment [138, 139]. Given the complexity of protein adsorption and cell–surface interactions, optimizing surface properties to achieve a balance between hydrophilicity and other surface features may help mitigate thrombosis risk and improve long-term performance, but further mechanistic and in vivo studies are needed to fully elucidate these effects.

In summary, morphological characterization of bioprosthetic valve tissues, from the macroscale to the nanoscale, is essential for understanding structural valve degradation and enhancing valve performance. Features such as surface roughness, fibrillar density, and microstructural integrity strongly influence the mechanical response of these tissues under loading. Consequently, this information is crucial for accurately characterizing their mechanical properties.

4.3 | Mechanical Testing

A crucial aspect—particularly for bioengineered aortic valves designed to address SVD—is the precise determination of the mechanical properties of the pericardial tissue, including hardness, elastic modulus, toughness, and tensile strength. Several experimental techniques are employed to characterize these properties, as described below.

4.3.1 | Nanoindentation

Nanoindentation is a powerful technique that enables the local measurement of mechanical properties, such as hardness and elastic modulus, with high spatial resolution [140]. The choice of indenter tip geometry depends on the material's characteristics: for hard biological materials, Berkovich or cubic tips are generally preferred, whereas for softer biological tissues, flat punch or spherical tips are more appropriate [141–145].

Nanoindentation has been successfully applied to characterize cardiovascular tissues, including aortic tissue, providing valuable insights into their local mechanical behavior [146–148]. However, given the intrinsic microstructure of these biological tissues, special care must be taken when interpreting results. In the case of cardiovascular tissue, the structure of the collagen fiber network plays a critical role in nanoindentation measurements. Because the size of the indenter tip is comparable to the dimensions of collagen fibrils, the interaction between the tip and the material deviates from the ideal assumptions underlying classical Hertzian contact mechanics theory [149]. This complicates the interpretation of the measured mechanical properties.

To address this, it is essential to perform indentation tests across a broad range of experimental conditions. For instance, Zhang et al. conducted dynamic nanoindentation on arteries subjected to varying pre-strain levels and loading directions, demonstrating that both storage and shear moduli increased with strain [150]. This was likely due to the reorganization of collagen fibrils under strain. Additionally, the viscoelastic relaxation behavior of the tissue decreased as the strain increased, indicating strain-dependent changes in the tissue's microstructure.

Similarly, bovine and porcine pericardium have been investigated using nanoindentation, although detailed methodological studies remain limited. A notable example is the work by Tobaruela et al., who performed fatigue nanoindentation by applying approximately 1500 indentation cycles to bovine pericardium [151]. Their findings revealed an 18% decrease in hardness after cycling, suggesting that early reductions in hardness could correlate with long-term fatigue behavior. This highlights the potential of nanoindentation fatigue tests as efficient preliminary assessments prior to more time-consuming fatigue experiments.

Given the complex microstructure of the pericardium and cardiovascular tissues in general, more comprehensive nanoindentation studies are warranted. Specifically, the influence of tissue morphology and the selection of indenter tip geometry on the measured mechanical properties need to be systematically investigated, as has been shown for more rigid materials [152]. That said, nanoindentation provides only localized information on the tissue and should therefore be complemented with mechanical property data obtained at the macroscale. In this context, greater attention should be directed toward techniques that enable noninvasive characterization of these properties.

4.3.2 | Acoustic and Ultrasound Investigation

Among the noninvasive techniques available for probing the mechanical properties of biological tissues, the use of acoustic waves stands out due to its versatility and sensitivity. Thanks to their capacity to operate across multiple length scales, acoustic-based methods have been increasingly employed to characterize non-standard and biological materials, including living muscles, soft tissues, and cardiovascular structures [153–155].

A key advantage of acoustic wave techniques lies in their scalability. They can probe mechanical properties from micrometer-scale resolutions, as in Scanning Acoustic Microscopy (SAM), to centimeter-scale measurements using pulse/receiver systems coupled with oscilloscopes [156, 157]. Additionally, sample preparation is minimal and nondestructive, often requiring only immersion in a coupling fluid or the ultrasound gel.

Notably, ultrasound-based methods have demonstrated greater consistency in estimating elastic constants compared to traditional mechanical testing (discussed later). For instance, Nowak et al. showed that ultrasound measurements in food samples yielded lower variability in stiffness values compared to standard tensile or compression tests [158].

However, careful consideration of sample geometry and anisotropy is critical. For example, accurate determination of the elastic moduli in cortical bone requires measurements at multiple orientations to account for directional dependencies [159]. Similar concerns apply to soft tissues such as the pericardium, which are highly heterogeneous and anisotropic due to their layered collagen architecture [112, 160, 161].

Moreover, while these methods are experimentally straightforward, they typically require significant computational effort and sophisticated modeling for data interpretation [162]. This is because the relationship between wave propagation and material properties is complex and often nonlinear, particularly in heterogeneous or anisotropic media. Additionally, conventional acoustic models do not inherently account for structural heterogeneity or laminar composition, which can lead to artifacts or misinterpretations in results (especially in layered tissues like the aortic valve leaflets).

For these reasons, a complete mechanical characterization of the tissue also requires the use of destructive techniques, such as tensile testing.

4.3.3 | Tensile Tests

Tensile testing represents one of the most fundamental techniques for characterizing the mechanical behavior of valve tissues. These tests yield key mechanical parameters such as Young's modulus, ultimate strength, strain at failure, and toughness, which are critical for informing computational models and improving valve design. For example, it is well-documented that cardiovascular tissues generally become stiffer with age [163].

Tensile testing also facilitates a more patient-specific approach to valve design, as the mechanical properties of valve tissue exhibit significant inter-patient variability [164]. Consequently, the materials used to fabricate bioprosthetic valves should ideally match the mechanical characteristics of the patient's native tissue [165]. While porcine and bovine pericardium are commonly considered optimal sources for aortic valve replacements, it is crucial to consider the age of the animal donor, as this factor significantly impacts tissue mechanical performance [166].

Thus, selecting the pericardial tissue is a crucial step in valve fabrication, but equally important is the method by which its mechanical properties are evaluated. Table 2 compiles recent tensile testing protocols for pericardium tissue, revealing significant heterogeneity in methodologies. While sample size appears to

TABLE 2 | Tensile test parameters used to characterize the pericardium membrane and polymeric films used for prosthetic valves.

Refs.	Membrane type	Length (mm)	Width (mm)	Speed (mm/min)
[169]	Human	10	7	10
[165]	Porcine, bovine			12
[167]	Porcine	21, 30	3, 5	1, 12, 50
[166]	Porcine, bovine	30	3	50
[126]	Bovine	12.5	2.27	20
[98]	Porcine, bovine	4	2	12
[112]	Porcine, bovine	10	2.3	20
[170]	Polymeric		2.5	1.5
[84]	Porcine	5	1	10
[38]	Bovine	12	2	20
[77]	Porcine	30	10	20
[124]	Bovine	35	6	50
[79]	Porcine	40	10	12.5
[160]	Polymeric			50
[81]	Bovine	35	5	10
[171]	Bovine	20	4	30
[83]	Porcine	20	10	10

have minimal impact on results [167], more evidence is needed in this regard, for the dimension of the bioprosthetic valve leaflets might have an impact on their durability. The strain rate at which tests are conducted plays a critical role due to the viscoelastic nature of the tissue [168]. Based on the literature, a strain rate of approximately 10–12 mm/min is generally appropriate for testing pericardium, consistent with protocols used for other cardiovascular tissues.

Another notable source of variability is the pre-conditioning (or preload) of samples prior to testing. Unfortunately, when reported, the preload protocols vary widely between studies, limiting the comparability of mechanical data and diminishing their utility for quantitative numerical modeling.

In addition to the testing protocol, the directional dependence of tissue mechanical behavior is a key consideration. It is well established that aortic valve leaflets exhibit anisotropy: the circumferential direction is generally stiffer than the radial [172]. Therefore, bioprosthetic valves must be fabricated with pericardium oriented correctly to replicate the natural anisotropic mechanics of native leaflets. Moreover, valve leaflets comprise multiple layers with distinct mechanical properties. Campion et al. characterized the mechanical behavior of fibrous and serous layers of bovine pericardium, finding that these individual layers are stiffer and stronger than the intact membrane [112]. This suggests that future valve designs could be mechanically tuned by selectively incorporating different layers. Building on this layered concept, Guo et al. recently demonstrated improved mechanical and structural performance of a polymer-based aortic valve by mimicking the multilayered architecture of native tissue [160]. Such studies emphasize the potential for future research focused on layer-specific mechanics to inform the design of more durable bioprosthetic valves.

Complementary to uniaxial tensile testing, biaxial tensile tests are essential for capturing the complex, multiaxial mechanical behavior of pericardium tissue [173]. However, biaxial data for the pericardium remain limited in the literature, and standardized testing protocols are currently lacking. Biaxial testing can reveal asymmetries in tissue stiffness, which may be exacerbated in degraded tissue [172]. For instance, Pancheri et al. found that the maximum circumferential stress and Young's modulus are positively correlated with the presence of calcifications in cardiovascular tissue, highlighting the importance of such tests in pathological contexts [174].

To emphasize the inter-study variability and the need for standardized tensile testing protocols, Table 3 summarizes experimental measurements of the elastic modulus for bovine and porcine pericardial tissues used in prosthetic valves. Reported values span a broad range (from approximately 14 to 145 MPa across the cited studies), reflecting significant variability. As previously discussed, this dispersion likely arises from differences in donor age, tissue processing (e.g., glutaraldehyde crosslinking or decellularization), predominant fiber orientation within the specimens, and testing protocols.

Overall, tensile testing provides essential quantitative data to inform computational models and valve design [180]. However, since aortic valves operate under continuous cyclic loading, understanding tissue fatigue behavior is equally critical. Therefore, fatigue testing of pericardium tissue is a necessary next step for advancing bioprosthetic valve durability and performance.

4.3.4 | Fatigue Tests

Fatigue testing involves applying cyclic loads to a sample while precisely controlling the amplitude and frequency of the loading cycles. According to the ISO 5840–3:2021, the standard requires imposing a normotensive differential pressure of 100 mmHg across the closed aortic valve, for a minimum of 200 million cycles. The tested valve must be exposed to this pressure for at least 5% of the cycle, and conditions must be maintained for at least 95% of the cycles. It is important to note that this pressure refers to the test load applied to the valve during durability testing and does not correspond to the physiological forward-flow transvalvular pressure gradient across a healthy aortic valve, which is typically a few mmHg (often <5 mmHg) and exceeds 40 mmHg only in severe stenosis. Importantly, fatigue testing should be conducted under physiological conditions. This means that the valve or tissue must be tested in a hydrated environment at body temperature (around 37°C). These strict requirements make standard mechanical testers often inadequate for fatigue testing, as they cannot replicate the complex testing conditions prescribed by the standard.

TABLE 3 | Experimental values from the literature of the elastic modulus, reported as Mean ± SD, of different pericardial tissues used for prosthetic valves. Abbreviations in the right column are given in the form: Type of test, age of donor, main direction of fibers with respect to the testing direction. *n*: Number of specimens; N: Native tissue; Decel: Decellularized tissue; GA: Tissue treated with glutaraldehyde; Uni: Uniaxial tensile test; Bi: Equibiaxial tensile test; BCM: Brillouin confocal microscopy; YP: Young animal pericardium; AP: Adult animal pericardium; AF: Aligned fibers; TF transversal fibers; MF: Mixed fibers. N.A.: Information not available. The numbers were corrected to account for significative figures.

Bovine Pericardium				
Refs.	***n***	**Treatment**	**Elastic modulus (MPa)**	**Additional information**
[175]	10	N	27 ± 20	Uni, N.A., N.A.
[176]	6	N	40 ± 15	Uni, N.A., N.A.
	6	Decel	23 ± 20	
	6	GA	51 ± 10	
	6	Decel + GA	28 ± 3	
[165]	N.A.	GA	98 ± 40	Uni, YP, TF
[177]	6	Decel + GA	48 ± 20	Uni, YP, N.A.
[166]	10	GA	102 ± 30	Bi, YP, N.A.
	10	GA	111 ± 30	
[98]	6	N	19 ± 9	Uni, N.A., N.A.
	6	GA	87 ± 30	
[126]	6	GA	145 ± 30	Uni, N.A., AF
	6	GA	26 ± 20	Uni, N.A., TF
	6	GA	84 ± 10	Uni, N.A., MF
[112]	10	GA	47 ± 20	Uni, N.A., MF
[178]	3	N	30 ± 10	BCM + Uni, N.A., N.A.
	3	GA	32 ± 10	
	3	Decel + GA	43 ± 7	
[124]	7	Decel	78 ± 6	Uni, N.A., AF
	7	Decel + GA	131 ± 10	
[81]	7	Decel + GA	37 ± 1	Uni, N.A., N.A.
[171]	10	GA	29 ± 9	Uni, N.A., MF
	10	Decel + GA	45 ± 20	
Porcine pericardium				
Reference	***n***	**Treatment**	**Elastic modulus (MPa)**	**Additional information**
[167]	N.A.	N	133 ± 20	Uni, YP, N.A.
	N.A.	GA	47 ± 9	
[165]	N.A.	GA	79 ± 30	Uni, YP, TF
[166]	13	GA	120 ± 60	Bi, YP, N.A.
[98]	6	N	27 ± 20	Uni, N.A., N.A.
[112]	10	GA	81 ± 40	Uni, N.A., MF
[179]	N.A.	N	37 ± 3	Uni, N.A., MF
	N.A.	Decel	14 ± 1	
[84]	6	Decel	22 ± 1	Uni, N.A., N.A.
	6	Decel + GA	36 ± 1	
[83]	4	Decel	57 ± 5	Uni, N.A., N.A.
	4	GA	95 ± 5	

In this context, Paez and colleagues have developed an elegant fatigue testing system designed to mimic physiological conditions [181–183]. Their setup consists of a pipe system connected to a hydraulic unit equipped with sensors that continuously measure and record pressure, deformation, time, and energy. A piston within the pipe pressurizes a saline-filled environment, simulating physiological pressure cycles. Using this system, fatigue tests were performed on bovine and ostrich pericardium, yielding valuable insights that suggest short-term fatigue tests may be indicative of long-term fatigue behavior in bioprosthetic valves. However, these studies did not meet the ISO standard's requirement of 200 million cycles, and the fixation method used to secure the membrane to the pipe may have introduced tissue damage, potentially biasing results.

To overcome such limitations, several companies have developed specialized heart valve tester units that deliver controlled fatigue loading consistent with ISO 5840 requirements (e.g., HiCycle durability tester developed by the Vivitro labs, BDC labs, Dynatek labs, TA instruments, or Azo materials). For example, Dalgliesh et al. used one such device to evaluate the behavior of pericardial fatigue, applying a sinusoidal pressure load with an amplitude of 120 mmHg at a frequency of 1400 cycles per minute [98]. Similarly, Li et al. tested valves under accelerated fatigue conditions at approximately 1800 bpm with peak pressures of 100 mmHg [84]. Vella et al. applied cyclic loading at 10 Hz with peak pressures of 100 mmHg, although their tests were conducted at room temperature [68]. These examples illustrate the wide range of testing conditions currently used in the field, underscoring the urgent need for a standardized fatigue testing protocol that aligns with both physiological and regulatory requirements. Nevertheless, some of the findings from these studies, summarized in Figure 7, provide valuable insights into how the mechanical properties, hydrodynamic performance, and overall durability of pericardial tissue evolve over millions of fatigue cycles.

Given that the pericardium is a viscoelastic material, the influence of test frequency on mechanical response deserves further investigation. Physiological heart rates range from 60 to 120 beats per minute (bpm), significantly lower than the frequencies used in accelerated fatigue testing. Understanding how loading speed affects tissue behavior, especially in terms of progressive damage accumulation and of viscoelastic properties, is therefore essential for accurately predicting in vivo valve durability [184].

Another important aspect of fatigue testing relates to tissue damage tolerance. A recent study demonstrated the remarkable resilience of collagenous tissues to damage [38]. They attributed this resilience to the ability of collagen fibers to reorient during crack propagation, which enhances flaw tolerance. Building on these findings, we propose that fatigue testing of valve replacement materials should also include specimens with induced defects or cuts, in order to assess their damage tolerance under cyclic loading conditions. In addition, fatigue testing should be conducted across a representative range of tissue thicknesses, as this parameter is a recognized determinant of valve durability [185, 186].

In conclusion, fatigue testing provides critical insight into how pericardium tissue responds to the cyclic mechanical demands inherent to aortic valve function. However, while fatigue and standard tensile tests offer valuable macroscopic mechanical data, they do not reveal material behavior at the micro- or nanoscale—a scale at which early structural valve deterioration processes likely originate. To address this gap, in situ techniques such as nanoindentation are required to investigate mechanical properties at smaller length scales and improve our understanding of valve degeneration mechanisms.

To conclude the section on multiscale physical characterization of the pericardium, we emphasize that an in-depth experimental understanding of the mechanical and structural properties of bioprosthetic aortic valve leaflets is not only essential for evaluating performance but also for informing the rational design of next-generation biomaterials. A truly multiscale characterization approach (linking molecular, microstructural, and macroscopic levels) is indispensable for deciphering the structure-function relationships in collagen-based or collagen-inspired systems.

Nevertheless, experimental techniques alone offer only a partial perspective. To overcome their inherent limitations, it is imperative to integrate experimental findings into advanced computational models. Such models can bridge scales, account for complex geometries and loading conditions, and ultimately guide the optimization of biomaterial design and functionality in clinically relevant scenarios.

5 | Computational modeling of SVD

The function of bioprosthetic aortic valves depends on the interplay between blood flow and leaflet mechanics, which makes computational modeling an important tool to study SVD. Most approaches rely on fluid–structure interaction (FSI), where Computational Fluid Dynamics (CFD) describes blood flow, and Finite Element Analysis (FEA) quantifies leaflet deformation and stress [187–190].

FEA is highly relevant to SVD because it quantifies leaflet stress distributions, which are closely linked to both calcification and fatigue. In this sense, stress concentrations and the accuracy of numerical models strongly depend on how tissue properties are defined [191, 192]. For example, changes in mechanical properties or the presence of structural heterogeneities, which can be introduced by fatigue damage or calcifications, can alter stress predictions by up to 40% [82, 193–195]. Similarly, mesh and boundary conditions have a critical influence on simulation outputs, especially near the valve–tissue interface, where fatigue damage often initiates [196]. Thus, the precise location of leaflet heterogeneities is crucial, for it significantly alters stress distribution on valve leaflets and also hemodynamics [197] (Figure 8a).

Over the decades, patient-specific modeling has significantly improved the precision of simulations by integrating medical imaging and FEA/CFD [199], which is relevant for simulating SVD. For instance, micro-CT enables the accurate representation of calcified regions, which can directly link simulation outcomes to the mechanisms of SVD [129]. Capturing positioning effects

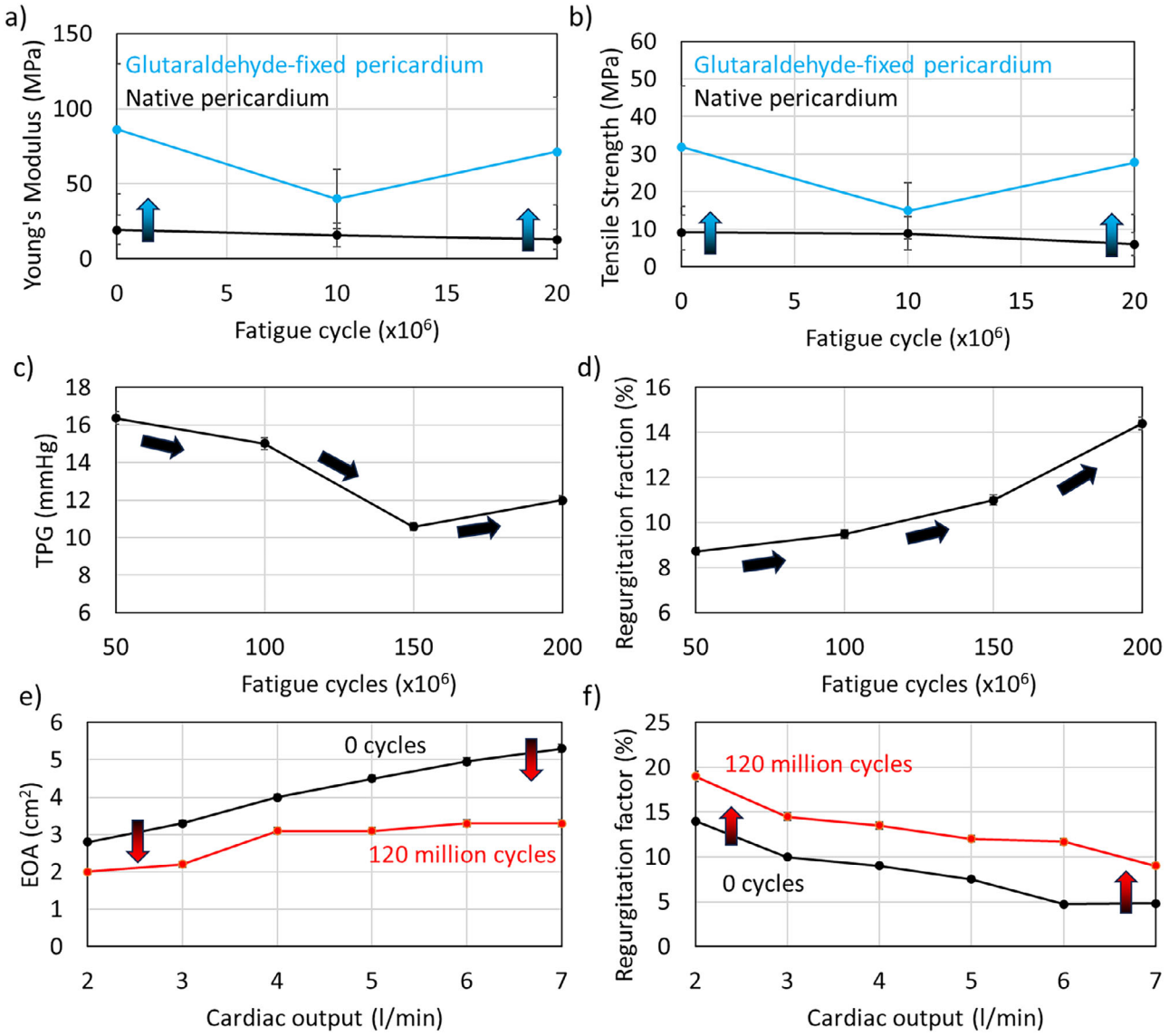

FIGURE 7 | Effects of fatigue on the biomechanical behavior of pericardial tissue and bioprosthetic valves. Evolution of (a) Young's modulus and (b) tensile strength of native and glutaraldehyde-fixed bovine pericardium as a function of fatigue cycles. Data from [98]. Changes in (c) transvalvular pressure gradient (TPG) and (d) regurgitation fraction during accelerated fatigue testing of bioprosthetic valves. Data from [84]. Variation of (e) effective orifice area (EOA) and (f) regurgitation fraction with increasing fatigue cycles. Data from [68].

also matters to better understand SVD, for valve misalignment can alter hemodynamics and leaflet stresses, which can accelerate leaflet degradation [200].

A critical contributor to SVD is the condition of the valve leaflet surface. Increased surface roughness enhances local turbulence, elevates shear stress on the pericardial tissue, and accelerates both mechanical damage and calcification [130, 133, 201]. Predicting these effects is challenging, as even small geometric deformations can significantly alter hemodynamics [202, 203]. For instance, leaflet fluttering has been observed to occur in flow regimes where transitional or disturbed flow develops; however, the relationship between fluttering, flow instabilities, and subsequent tissue damage or calcification remains unclear [198, 204] (Figure 8b). From a structural mechanics perspective, fluttering is further amplified by stiffness heterogeneities, such as localized calcifications or tissue damage [205, 206].

Recent advances in computational modeling increasingly leverage fully coupled FSI frameworks to investigate the interplay between hemodynamic forces, leaflet mechanics, and early indicators of calcific degeneration. Experimental–computational studies have shown that early-stage calcification is associated with measurable changes in hemodynamic biomarkers, particularly time-averaged wall shear stress [207], while FSI simulations have demonstrated that leaflet flutter amplifies oscillatory shear, residence time, and endothelial activation potential, linking local flow–structure interactions to mechanisms promoting mineral accumulation [204]. High-fidelity FSI analyses have further highlighted how valve architecture and coupled flow–structure dynamics govern turbulence, energy transfer, and mechanical loading patterns relevant to long-term degeneration [208, 209]. Patient-specific computational studies have quantitatively linked post-implantation hemodynamic indices to long-term structural valve deterioration [210].

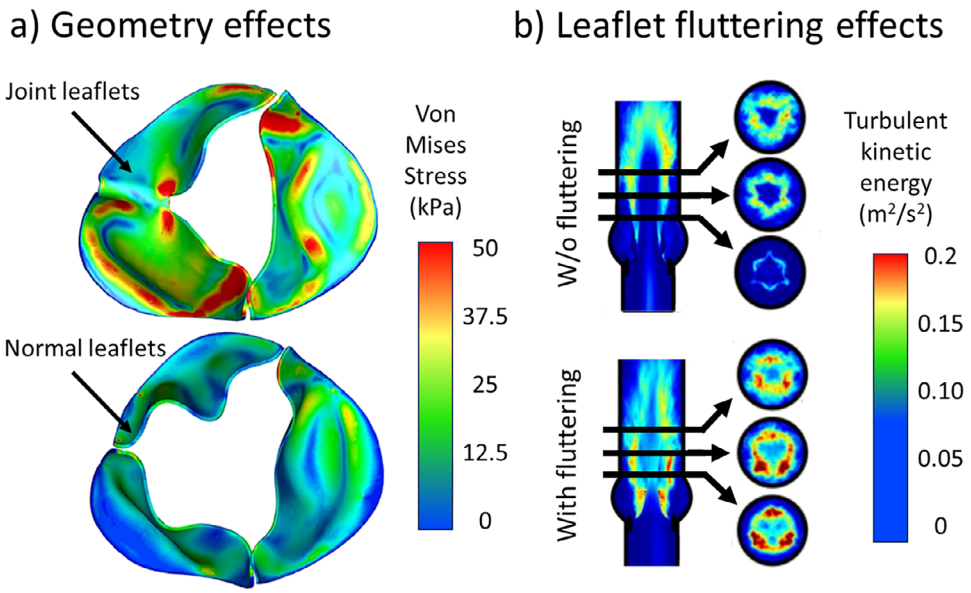

FIGURE 8 | (a) Effects of small geometrical differences on the stress the leaflets experience during opening and closing under pre-determined flow conditions. Leaflets with altered geometries (e.g., thicker, calcified) can lead to substantial differences in stress concentrations. The data used to produce this figure were taken from [197]. (b) The presence of leaflets fluttering affects the turbulence level of the blood flow. The presence of turbulent flows can induce damage and lead to SVD. Adapted with permission from [198], AIP Publishing, 2026.

Within this context, validation of FSI-derived calcification risk metrics can be viewed as a progressive roadmap, spanning explant-level, in vitro, and in vivo evidence. Multiscale and multimodal characterization of failed bioprosthetic valve explants has shown that mineralization patterns colocalize with regions exposed to elevated hemodynamic and biomechanical stresses predicted by simulations, providing mechanistic validation at the tissue level [74]. At the in vivo scale, advanced imaging modalities such as PET-CT (Positron Emission Tomography) have demonstrated the ability to detect subclinical bioprosthetic degeneration and predict subsequent valve dysfunction, establishing clinically relevant imaging biomarkers of calcific progression [211]. Complementarily, patient-specific FSI models validated against in vitro flow measurements and in vivo imaging data have shown accurate reproduction of pre-intervention hemodynamics, supporting the translational integration of computational predictions into clinical assessment frameworks [212]. In some cases, valve distortion occurs due to the interaction between the native aortic valve and the implanted bioprosthetic valve [213]. Although it is often assumed that the presence of the native valve has minimal impact on bioprosthetic function [214], this interaction is rarely modeled explicitly. The residual native tissue may introduce asymmetries or more compliant boundary conditions, which alter the stress distribution [195]. For instance, Sturla et al. showed that local stent distortion during implantation is due to calcified native tissue and can cause leakage and disturbed hemodynamics [215]. However, a limitation of that study was its focus on tissue-level stress–strain behavior, without accounting for the microstructural architecture of the valve leaflets, which could significantly influence damage progression.

At the microstructural level, the effects of crimping the valve before deployment are often overlooked. Bressloff found that crimping causes localized stress concentrations that follow the geometry of the stent and the skirt [216]. These stresses, often above several MPa, are sufficient to plasticize collagen, which could initiate localized damage zones. Although mesh resolution may overestimate these stress levels [196], they nonetheless suggest a need to investigate how micro-plasticized regions influence the fatigue life of the valve, for example, by incorporating geometrically defined damage into simulations.

Among the various SVD mechanisms, fatigue of the leaflets is widely accepted as one of the most critical factors, even in non-calcific valves. Martin and Sun showed that heterogeneous elastic properties, poor leaflet coaptation, and limited stent-tip deflection can accelerate fatigue-related degradation [217]. Their findings were based on parametric FEA studies that varied the biaxial stress distribution in the leaflets, mimicking the softening behavior of biological tissues under repeated loading.

Fatigue not only weakens the tissue but also alters stress distribution patterns within the valve. This means that regions most prone to failure may not correspond to those with the highest initial stress in a non-fatigued state. Smith and co-workers observed that fatigue leads to plastic deformation of the leaflets, often resulting in sagging [218]. This sagging alters the curvature of the leaflet, reducing its ability to dissipate stress. Moreover, these sagged regions were found to correlate with distorted collagen fiber orientation, further compromising mechanical performance.

The influence of geometry on durability has also been investigated through finite element models. Dabiri and Narine, using a Fung-type orthotropic material model, showed that a parabolic radial curvature and downward leaflet inclination in the closed configuration are associated with longer bioprosthetic valve lifespan [219].

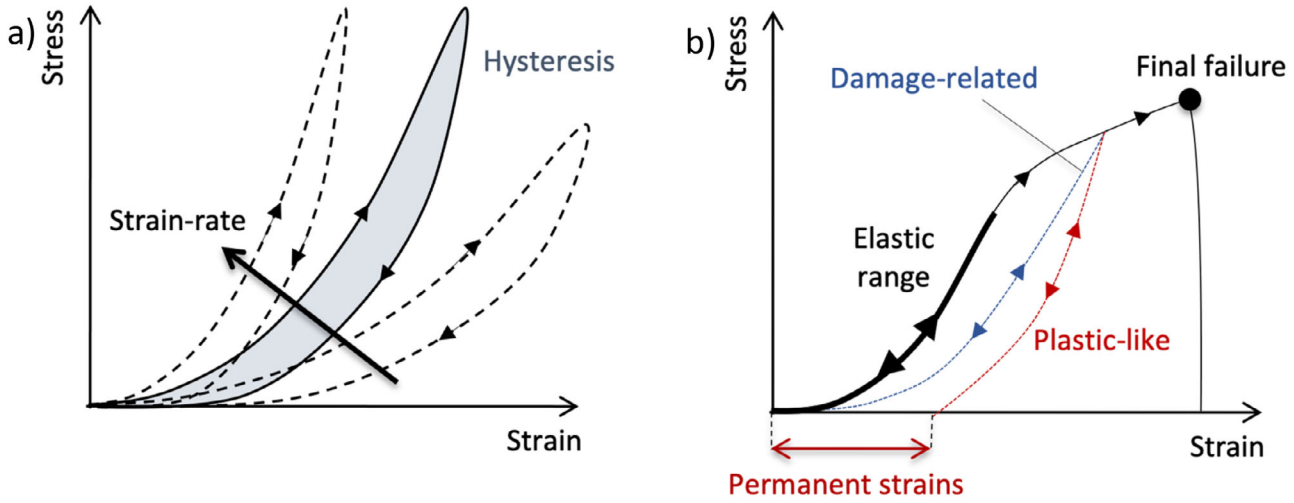

FIGURE 9 | Inelastic behavior of soft tissues. (a) Rate-dependent viscous response with hysteresis. (b) history-dependent damage, plastic-like permanent strain, and failure.

In terms of computational modeling, FEA has been used to simulate bioprosthetic valves under hundreds of millions of fatigue cycles [161]. In this work, the authors found that the valve base (the suture attachment region) fails primarily due to fatigue, while leaflet contact regions degrade due to a combination of fatigue and wear from repeated contact, a process that may be exacerbated by calcification.

Simulating the effects of fatigue realistically remains a computationally intensive task. To represent real-world fatigue conditions, models should ideally account for over 200 million cycles, posing significant numerical challenges. Moreover, accurate modeling requires consideration of local variations in mechanical properties, which further increases the computational load.

5.1 | Constitutive Modeling Principles for SVD

Because SVD arises from multiple inelastic processes, its modeling requires integrating complementary constitutive principles that extend beyond purely hyperelastic laws. In particular, the tissue state is generally described by observable measures (e.g., strain) and internal variables representing latent microstructural processes (e.g., plasticity or damage)—each evolving under thermodynamic consistency [220]. This framework is especially relevant for bioprosthetic valve leaflets, which experience combined tensile, flexural, and shear stresses under cyclic opening, closure, and transvalvular loading, with collagen fibers providing the primary structural reinforcement governing load transfer and durability. In this context, the major ingredients used to reproduce inelastic effects in soft tissues are depicted in Figure 9 and discussed as follows.

Viscoelasticity captures rate-dependent behavior such as hysteresis and stress relaxation by coupling viscoelastic branches to an anisotropic hyperelastic matrix (e.g., quasi-linear viscoelasticity or Maxwell-type models) [221]. The identification of the relevant parameters relies on relaxation and dynamic mechanical tests. Experimental imaging studies have shown that cyclic loading induces time-dependent reorientation of collagen fibers, indicating that viscoelastic responses are intimately linked to evolving fiber architecture rather than purely matrix-driven effects [222].

Progressive damage models describe the gradual stiffness loss and permanent set observed under cyclic loading. Internal variables degrade stiffness once strain or energy thresholds are exceeded, reproducing the softening and residual stretch seen experimentally [223]. Time-evolving constitutive modeling has shown that, in pericardial xenograft tissues used for bioprosthetic heart valves, cyclic loading induces plastic-like strains and permanent geometric changes during the early in vivo period, leading to spatially heterogeneous curvature and stress redistribution without immediate structural failure [224].

In contrast to progressive degradation, discontinuous damage arises in two distinct forms. The first form includes localized failures such as delamination or tearing, typically modeled via cohesive-zone or phase-field formulations. In this context, calcification amplifies these effects by creating sharp stiffness mismatches that promote stress concentration and microcrack nucleation [225, 226]. The second form of discontinuous damage occurs when collagen fibers lose their crimp after exceeding prior load maxima, producing stepwise, load-memory-driven degradation [227, 228].

As discussed in the previous sections, permanent deformations arise from plastic-like sliding of collagen fibers or matrix rearrangements, leading to residual strains that alter subsequent stress fields [220, 229]. Valve-level simulations incorporating time-evolving tissue constitutive laws have demonstrated that such permanent deformations are accompanied by anisotropic regional changes in collagen fiber orientation and recruitment, which in turn modify local stiffness and stress–strain behavior [224]. Plasticity often couples with damage evolution, influencing fatigue and long-term durability. The effects of permanent deformations can be captured by introducing inelastic strain variables that evolve once stresses exceed a threshold.

Fatigue models address cumulative degradation under millions of cardiac cycles [230, 231]. Energy-based formulations describe

gradual microstructural weakening, while crack-growth laws capture discontinuous fatigue. Because collagen fiber recruitment increases with cyclic loading and places an upper bound on plastic strain, fiber architecture acts as a limiting mechanism for further geometric evolution, thereby directly influencing fatigue susceptibility and long-term durability [224]. Calcification lowers the endurance limit by creating early crack nucleation sites and amplifying cyclic stress amplitudes. Because simulating billions of cycles is infeasible, accelerated cycle-jump or surrogate approaches are used to retain mechanistic fidelity.

Chemical–mechanical coupling accounts for how fixation and in vivo chemistry modify collagen properties. Crosslink density and glycation alter stiffness and damage thresholds, linking biochemical changes to mechanical degradation. Constitutive models can capture this by letting fiber stiffness or damage thresholds depend on crosslink density, thereby linking chemistry to mechanics and damage or fatigue progression [95].

Taken together, these inelastic mechanisms provide a multiscale constitutive framework for simulating SVD. By integrating viscoelasticity, damage, fatigue, and chemical coupling, and cyclic-loading-induced changes in collagen fiber recruitment and orientation, computational models can reproduce the coupled mechanical and biochemical pathways that govern structural valve deterioration and inform material design for next-generation bioprosthetic valves.

5.2 | Future Steps in Computational Modeling of SVD

One of the major challenges in modeling SVD is the computational cost associated with standard simulation practices. Most current models rely on 3D or 2D geometries with full mechanical solvers, which are computationally intensive, particularly when coupled with FSI or long-term fatigue simulations.

To address this, Lopez and co-authors analytically predicted the forces at the interfaces between the valve leaflets and the blood [232]. This prediction was crucial for defining common time steps (i.e., discrete time increments used to advance the simulation) for both the Lattice Boltzmann Method (LBM) and Finite Element Method (FEM). By aligning these time steps, the authors significantly simplified the fluid–structure interaction (FSI) computations.

To further reduce the computational cost associated with FSI problems, Reduced Order Modeling (ROM) techniques offer a promising approach. These methods simplify high-fidelity models by decreasing their computational complexity while preserving the essential physical behavior of the system. ROMs are typically built either from physical or mathematical principles that describe the system's behavior, or from data-driven methods that learn reduced representations directly from simulation or experimental data [233]. This methodology has been successfully applied to the study of bioprosthetic and native valve regurgitation [234]. However, such reduced models inherently simplify the system and may neglect important details, which limits their suitability for fully patient-specific analyses.

Also, for reducing computational cost, Fumagalli et al. proposed an innovative lumped-parameter model to study aortic valve FSI [235]. In their approach, valve stenosis was modeled by increasing stiffness parameters, and calcification was represented by increasing leaflet inertia. This significantly reduced computational cost compared to full CFD or FEA simulations. However, this simplification comes at the expense of realism: the model cannot capture local deformations, leaflet coaptation, prolapse, or heterogeneity in material properties, which are factors that often require full 3D representations. That said, it is important to note that addressing specific phenomena such as leaflet flutter requires adequate spatial and temporal resolution. In particular, reliable analysis demands flow resolutions on the order of ~50 μm, structural resolutions of ~250 μm, and temporal sampling rates of at least 1000 Hz to accurately capture flutter dynamics.

Additionally, the model does not account for the evolution of calcified tissue, a critical component of SVD. To address this gap, we propose that the values reported in Table 1 (or future experimental datasets) could be used to establish analytical laws governing the progression of calcification over time. In this context, Tsolaki et al. [74] proposed a predictive model linking local flow-induced stresses and tissue deformation to calcification development, accounting for approximately 74% of the experimentally observed variability. The importance of robust analytical and constitutive models in improving numerical simulations has been strongly emphasized in previous works [236].

For instance, new fatigue-specific constitutive models for soft tissues could be developed and integrated into simulation frameworks [230]. These models would ideally be grounded in experimental data derived from advanced testing techniques, such as nanoindentation, which has already shown promise in evaluating tissue fatigue properties at the microscale [151, 182].

An important but still underexplored direction is the modeling of pericardial structure and morphology. As shown, the pericardium is composed of multiple layers, each with distinct mechanical properties [4, 112]. Accurately capturing these layers in numerical models is critical for understanding fatigue behavior. Moreover, such structural heterogeneity influences tissue remodeling under mechanical load, thereby affecting both valve function and long-term durability [64].

Future FEA and CFD studies should also account for geometric asymmetries, particularly those introduced by the interaction between native and bioprosthetic valve structures. Even slight misalignments, such as those of the native leaflet relative to the prosthetic skirt, can result in a 40% change in hemodynamic performance [237]. This underscores the need for more geometrically precise models, especially at critical interfaces like the suture and stent-pericardium junctions.

Thus, to build more realistic and predictive models of SVD, several improvements are essential: (1) enhanced geometric accuracy, especially around sutures and attachment points, to better capture the mechanics at the stent-tissue interface; (2) microscale simulations focused on fatigue behavior at stent anchoring points; (3) improved implementation of mechanical properties in bioprosthetic materials, based on

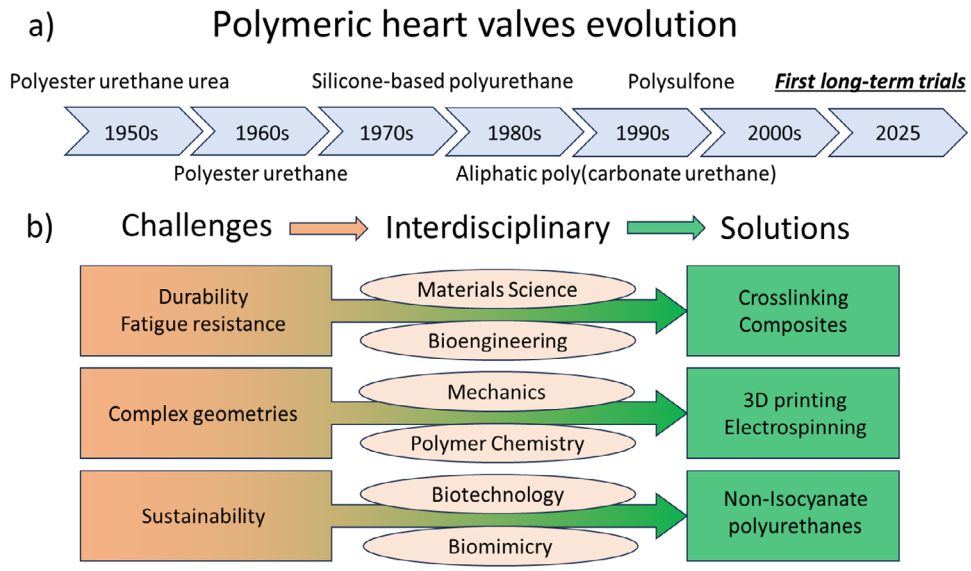

FIGURE 10 | (a) The evolution of the materials used for polymeric heart valves has constantly evolved till the most recent results for the long-term clinical trials in humans. Since their first conceptualization, it took roughly 70 years to achieve clinical solutions. (b) The main challenges that limit the use of polymeric heart valves highlight the importance of fundamental interdisciplinary work.

high-quality experimental data; (4) routine material property and mesh sensitivity analyses studies to ensure robustness and reproducibility; (5) development of reduced lumped -parameter models as complementary tools to reduce simulation time and cost without entirely sacrificing key mechanical insights.

In summary, while high-fidelity FSI and FEA simulations remain the gold standard, their future success in modeling SVD will rely on integrating experimental insights, microstructural realism, and efficient modeling strategies. By combining detailed material data with scalable numerical methods, the field can move toward more predictive, personalized, and clinically relevant computational tools, thus reducing SVD.

6 | A Glimpse Into Polymeric Heart Valve Development

While pericardium remains the most widely used material for fabricating prosthetic heart valves [238], growing interest is being directed toward synthetic polymeric valves due to their potential advantages in sustainability, processability, and scalability [46]. Since their early conceptualization in the 1950s [239], polymeric heart valves have undergone significant technological evolution, culminating in their recent entrance into clinical trials (Figure 10a). A multicenter in vivo study on a polymeric surgical mitral valve implanted for one year demonstrated encouraging results, reporting stable hemodynamic performance and good biocompatibility [240].

It is important to emphasize that polymeric and bioprosthetic heart valves undergo fundamentally different degradation and failure mechanisms. In bioprosthetic tissues, degeneration is largely driven by calcification processes involving residual cellular components, aldehyde-mediated calcium binding, and host-mediated biological responses [53, 67, 72]. In contrast, polymeric valves are primarily affected by physicochemical aging mechanisms such as oxidative degradation, chain scission, fatigue crack initiation, and protein-mediated surface alterations [241]. Consequently, the two classes of materials should not be considered mechanistically equivalent.

Nevertheless, polymeric valves face analogous engineering challenges, particularly with respect to long-term durability, fatigue resistance under cyclic loading, and preservation of mechanical function under physiological conditions. Addressing these challenges has driven decades of material innovation, spanning from early silicone-based devices to modern polyurethanes and composite polymers [242]. Despite the progress, critical challenges remain before widespread clinical adoption, including improving durability, reducing cost, and ensuring long-term biocompatibility. In this context, advances in polymer chemistry and material science are key drivers of innovation [100, 243] (Figure 10b).

For instance, Melo and collaborators recently introduced a polymeric valve based on non-isocyanate polyurethanes, designed with a focus on sustainability [244]. Their in vitro study reported no signs of calcification over an 8-week period, along with hemodynamic performance comparable to that of standard bioprosthetic valves.

Matching the mechanical properties of native valve tissues remains a fundamental design goal. Hydrogels have shown promise due to their tissue-like elasticity and viscoelasticity; however, their fabrication methods often make it difficult to replicate the complex leaflet geometry required for physiological function [47]. This is particularly important because reducing leaflet stress through careful geometrical design is essential for long-term durability [46].

A promising strategy involves the development of multilayered leaflets to enhance fatigue resistance [241]. Techniques such as

electrospinning and the use of ultrahigh molecular weight polymers can facilitate the creation of such hierarchical structures. However, in fiber-based materials, fiber orientation plays a crucial role in fatigue performance and must be carefully controlled [245].

Innovations in 3D printing also hold great promise, offering the possibility of fabricating valves with complex architectures tailored to patient-specific anatomy and mechanical requirements [246]. These technologies can enable the integration of multiple materials, mimicking the heterogeneous structure of native leaflets. Comparative studies of native tissue structures remain essential to inform the design of these synthetic alternatives, e.g., by elucidating how individual leaflet layers contribute to fatigue resistance [245]. These comparative studies aim to inform structural design principles to improve stress distribution and damage tolerance, rather than implying mechanistic equivalence.

Moreover, emerging material architectures such as auxetic structures (materials with a negative Poisson's ratio) are gaining attention in the context of valve design. Auxetic materials exhibit a counterintuitive property, becoming thicker perpendicular to the applied force, which can inhibit crack propagation under tensile loading, thereby offering enhanced tear resistance [247–250].

Incorporating nanomaterials as reinforcing fillers is another active area of research. While nanofillers can significantly improve mechanical properties, they also introduce challenges related to dispersion, matrix bonding, and biocompatibility [251]. Achieving uniform dispersion under mild processing conditions, while maintaining the sustainability of the material system, is particularly demanding [252–256].

As discussed in previous sections, the presence of dense networks of hydrogen bonds has been shown to improve fatigue resistance in polymeric materials. This feature is more easily tuned in synthetic systems through the use of commercial crosslinkers, particularly in polyurethane matrices [170, 257].

Ultimately, one of the most significant and still unmet goals in polymeric heart valve development is to endow them with self-healing, remodeling, and regenerative capacities. Achieving this will likely require the integration of multiple strategies, drawing inspiration from both synthetic and bioprosthetic systems, while recognizing the fundamental differences between synthetic and biological systems [258].

7 | Durable Bioprosthetic Aortic Valves—The Path Forward

Achieving durable bioprosthetic aortic valves requires coordinated progress across clinical practice, material science, and computational modeling.

On the clinical side, timely and accurate staging of SVD is critical to guide interventions. Harmonizing the quantitative criteria used to define SVD stages will enhance consistency across studies and improve long-term patient monitoring.

From a materials perspective, long-term bioprosthetic valve degeneration arises from the complex interplay between calcification and fatigue-related microstructural changes. Cyclic loading induces fiber recruitment, unfolding, and Mullins-like softening, which progressively weaken the tissue, while calcification locally stiffens leaflets and alters stress distributions. The relative contributions of these mechanisms remain difficult to quantify, as they often act synergistically. This complexity underscores the need for standardized experimental protocols. These should include reliable methods for quantifying calcium deposition, fatigue testing under physiological conditions, and tensile testing of pericardial tissue. Emerging techniques—such as nanoindentation and acoustic-based measurements—can provide detailed insights into tissue mechanics, offering essential data for refining predictive models.

A major open question remains how collagen damage propagates across hierarchical scales in bioprosthetic pericardium, from molecular disruptions of the triple helix to fibril shearing, fiber slippage, and tissue-level delamination. These multiscale failure mechanisms are modulated by fixation chemistry (e.g., glutaraldehyde), which alters local biochemical environments and mechanical thresholds [74]. Understanding how these factors interact is crucial for unraveling the inelastic and fatigue behavior of biological valve tissues.

To capture such complexity, computational models must evolve to integrate experimental insights across length scales. This requires a shift from purely elastic formulations to constitutive models that account for inelastic phenomena such as stress softening, permanent set, cyclic damage, and chemical–mechanical coupling. Promising approaches include progressive damage models, multiphase fiber recruitment, and fatigue-informed plasticity frameworks. Embedding these into valve-level simulations will improve our ability to predict failure modes under physiological loading and assess long-term durability.

These insights can directly inform the design of bio-inspired prosthetic valves, combining the multilayered structure of native pericardium with advanced manufacturing techniques such as 3D printing and electrospinning. The integration of standardized material characterization and multiscale modeling emerges as a central strategy to prevent SVD and enhance device performance.

To accelerate both scientific progress and clinical translation, we identify five key priorities for the field: (1) elucidate multiscale damage pathways through coordinated mechanical and biochemical investigations; (2) standardize testing protocols for fatigue, tensile strength, nanoindentation, and calcification to enable reproducible comparisons and model calibration; (3) develop microstructure-informed constitutive models that capture key damage mechanisms and reflect real-world material behavior; (4) incorporate geometry and constraint-specific effects into simulations, particularly at critical regions such as the stent–tissue interface; (5) balance model fidelity and computational efficiency by integrating high-resolution FSI/FEA tools with reduced-order or surrogate approaches.

By aligning experimental evidence, computational modeling, and clinical insight, this roadmap provides a foundation for the

rational development of next-generation bioprosthetic valves—devices engineered for longer-lasting performance and reduced risk of structural deterioration.

Acknowledgements

M.C., M.M., and G.G. were supported by the European Union—NextGenerationEU, Mission 4 Component 1, CUP E53C24002920006 (PRIN 2022 Program, Project 2022Z24WLR, Acronym: MATERIAL). GG is thankful to Dr. Alessandro Caimi for the suggestions and fruitful discussions. All the images were produced by the authors using original images or images under Gold Open Access with a Creative Commons Attribution (CC BY) license (these image parts were properly cited and acknowledged in the manuscript).

Funding

M.C., M.M., P.G., and G.G. were supported by the European Union—NextGenerationEU, Mission 4 Component 1, CUP E53C24002920006 (PRIN 2022 Program, Project 2022Z24WLR, Acronym: MATERIAL). M.C. acknowledges the support by Ricerca Corrente funding from the Italian Ministry of Health to IRCCS Policlinico San Donato and by the European Union (ERC, EPEIUS, 101125466). Views and opinions expressed are, however, those of the author(s) only and do not necessarily reflect those of the European Union or the European Research Council. Neither the European Union nor the granting authority can be held responsible for them.

Conflicts of Interest

The authors declare no conflicts of interest.

Data Availability Statement

All the data necessary to read and understand this manuscript are contained in the main file.

References

1. F. Saremi, *Revisiting Cardiac Anatomy: A Computed-Tomography-Based Atlas and Reference* (Wiley-Blackwell, 2011).

2. M. S. Sacks and A. P. Yoganathan, "Heart Valve Function: a Biomechanical Perspective," *Philosophical Transactions of the Royal Society B: Biological Sciences* 362 (2007): 1369–1391, https://doi.org/10.1098/rstb.2007.2122.

3. F. J. Schoen, "Evolving Concepts of Cardiac Valve Dynamics," *Circulation* 118 (2008): 1864–1880, https://doi.org/10.1161/CIRCULATIONAHA.108.805911.

4. A. Hasan, K. Ragaert, W. Swieszkowski, et al., "Biomechanical Properties of Native and Tissue Engineered Heart Valve Constructs," *Journal of Biomechanics* 47 (2014): 1949–1963, https://doi.org/10.1016/j.jbiomech.2013.09.023.

5. M. Avvedimento and G. H. L. Tang, "Transcatheter Aortic Valve Replacement (TAVR): Recent Updates," *Progress in Cardiovascular Diseases* 69 (2021): 73–83, https://doi.org/10.1016/j.pcad.2021.11.003.

6. B. R. Lindman, M.-A. Clavel, P. Mathieu, B. Iung, C. M. Otto, and P. Pibarot, "Calcific Aortic Stenosis," *Nature Reviews Disease Primers* 2 (2016): 16006, https://doi.org/10.1038/nrdp.2016.6.

7. M. J. Thubrikar, M. R. Labrosse, K. J. Zehr, F. Robicsek, G. G. Gong, and B. L. Fowler, "Aortic Root Dilatation May Alter the Dimensions of the Valve Leaflets☆," *European Journal of Cardio-Thoracic Surgery* 28 (2005): 850–855, https://doi.org/10.1016/j.ejcts.2005.09.012.

8. J. Zamorano, P. Lancellotti, L. Pierard, and P. Pibarot, *Heart Valve Disease: State of the Art* (Springer, 2020), https://doi.org/10.1007/978-3-030-23104-0.

9. J. I. E. Hoffman and S. Kaplan, "The Incidence of Congenital Heart Disease," *Journal of the American College of Cardiology* 39, no. 12 (2002): 1890–1900, https://doi.org/10.1016/S0735-1097(02)01886-7.

10. B. H. Lorell and B. A. Carabello, "Left Ventricular Hypertrophy," *Circulation* 102, no. 4 (2000): 470–479, https://doi.org/10.1161/01.CIR.102.4.470.

11. B. F. Stewart, D. Siscovick, B. K. Lind, et al., "Clinical Factors Associated With Calcific Aortic Valve Disease," *Journal of the American College of Cardiology* 29, no. 3 (1997): 630–634, https://doi.org/10.1016/S0735-1097(96)00563-3.

12. R. J. Everett, D. E. Newby, A. Jabbour, Z. A. Fayad, and M. R. Dweck, "The Role of Imaging in Aortic Valve Disease," *Curr Cardiovasc Imaging Rep* 9, no. 21 (2016), https://doi.org/10.1007/s12410-016-9383-z.

13. M. L. Brown, H. V. Schaff, B. D. Lahr, et al., "Aortic Valve Replacement in Patients Aged 50 to 70 Years: Improved Outcome With Mechanical versus Biologic Prostheses," *Surgery for Acquired Cardiovascular Disease* 135 (2008): 878–884, https://doi.org/10.1016/j.jtcvs.2007.10.065.

14. M. Kopytek, J. Tarasiuk, S. Wroński, et al., "Long-Lasting Rivaroxaban Use Is Associated With Lower Aortic Valve Leaflet Calcification in Severe Aortic Stenosis," *Canadian Journal of Cardiology* 41 (2025): 2027–2040, https://doi.org/10.1016/j.cjca.2025.06.068.

15. A. Kulik, P. Be, B.-K. Lam, et al., "Mechanical versus Bioprosthetic Valve Replacement in Middle-Aged Patients," *European Journal of Cardio-Thoracic Surgery* 30 (2006): 485–491, https://doi.org/10.1016/j.ejcts.2006.06.013.

16. D. S. Peterseim, Y.-Y. Cen, K. Landolfo, T. M. Bashore, J. E. Lowe, and W. G. Wolfe, "Long-Term Outcome after Biologic versus Mechanical Aortic Valve Replacement in 841 Patients," *The Journal of Thoracic and Cardiovascular Surgery* 117, no. 5 (1999): 890–897, https://doi.org/10.1016/S0022-5223(99)70368-5.

17. M. Casenghi, R. Gorla, A. Popolo Rubbio, et al., "One-Year Safety and Efficacy Profile of Transcatheter Aortic Valve-in-Valve.Pdf," *Catheterization and Cardiovascular Interventions* 98 (2020): E145–E152, https://doi.org/10.1002/ccd.29353Catheter.

18. S. J. Head, M. Celik, and A. Pieter Kappetein, "Mechanical versus Bioprosthetic Aortic Valve Replacement," *European Heart Journal* 38 (2017): 2183–2191, https://doi.org/10.1093/eurheartj/ehx141.

19. S. Kueri, F. A. Kari, R. A. Fuentes, H.-H. Sievers, F. Beyersdorf, and W. Bothe, "The Use of Biological Heart Valves," *Deutsches Ärzteblatt International* 116 (2019): 423–431, https://doi.org/10.3238/arztebl.2019.0423.

20. Y. Liu, C. Cheng, J. Xing, Z. Deng, and X. Peng, "Recent Advances and Practical Challenges in the Research of Decellularized Matrices for the Fabrication of Tiny-Diameter artificial Arteries," *Collagen and Leather* 7 (2025), https://doi.org/10.1186/s42825-025-00192-y.

21. P. G. Malvindi, S. Luthra, C. Olevano, H. Salem, M. Kowalewski, and S. Ohri, "Aortic Valve Replacement With Biological Prosthesis in Patients Aged 50 – 69 Years," *European Journal of Cardio-Thoracic Surgery* 59 (2021): 1077–1086, https://doi.org/10.1093/ejcts/ezaa429.

22. L. P. Dasi, H. Hatoum, A. Kheradvar, et al., "On the Mechanics of Transcatheter Aortic Valve Replacement," *Annals of Biomedical Engineering* 45, no. 2 (2017): 310–331, https://doi.org/10.1007/s10439-016-1759-3.

23. R. G. Nampi, L. Pospishil, and P. J. Neuburger, "TAVR versus SAVR for the Treatment of Aortic Stenosis: Do We Have a Clear Winner?," *Journal of Cardiothoracic and Vascular Anesthesia* 34, no. 8 (2020): 2100–2102, https://doi.org/10.1053/j.jvca.2020.04.013.

24. D. O'Hair, S. J. Yakubov, K. J. Grubb, et al., "Structural Valve Deterioration after Self-Expanding Transcatheter or Surgical Aortic Valve Implantation in Patients at Intermediate or High Risk," *JAMA Cardiology* 8, no. 2 (2022): 111–119, https://doi.org/10.1001/jamacardio.2022.4627.

25. T. Sharma, A. M. Krishnan, R. Lahoud, M. Polomsky, and H. L. Dauerman, "National Trends in TAVR and SAVR for Patients With Severe

Isolated Aortic Stenosis," *Journal of the American College of Cardiology* 80, no. 21 (2022): 2054–2056, https://doi.org/10.1016/j.jacc.2022.08.787.

26. M. I. Angela, "Pre-Dilation and Post-Dilation in Transcatheter Aortic Valve Replacement: Indications, Benefits and Risks," *Interventional Cardiology* 16, no. e28 (2021), https://doi.org/10.15420/icr.2020.35.

27. J. Li, Z. Meng, W. Yan, W. Wang, L. Wei, and S. Wang, "Computational Study of the Balloon Dilation Steps on Transcatheter Aortic Valve Replacement," *Frontiers in Bioengineering and Biotechnology* (2023): 1–9, https://doi.org/10.3389/fbioe.2023.1333138.

28. E. L. Keuffel, M. Reifenberger, A. Pellegrini, et al., "Economic Option Value Associated With Surgical Aortic Valve Replacement Using a Novel Bioprosthetic and a Future Transcatheter Aortic Valve-in-Valve procedure," *Journal of Medical Economics* 28, no. 1 (2025): 778–787, https://doi.org/10.1080/13696998.2025.2503664.

29. J. G. Almeida, S. M. Ferreira, and P. Fonseca, "Comparison of Self-Expanding and Balloon-Expandable Transcatheter Aortic Valves Morphology and Association With Paravalvular Regurgitation: Evaluation Using Multidetector Computed Tomography," *Valvular and Structural Heart Diseases* 92, no. 3 (2018): 533–541, https://doi.org/10.1002/ccd.27401.

30. S. Egron, B. Fujita, L. Gullón, et al., "Radial Force: an Underestimated Parameter in Oversizing Transcatheter Aortic Valve Replacement Prostheses: in Vitro Analysis With Five Commercialized Valves," *ASAIO Journal* 64, no. 4 (2018): 536–543, https://doi.org/10.1097/MAT.0000000000000659.

31. N. Satomi, M. Miyasaka, Y. Enta, et al., "Transcatheter Aortic Valve Replacement for Structural Valve Deterioration after Aortic Valve Neocuspidization," *Catheterization and Cardiovascular Interventions* 106 (2025): 610–620, https://doi.org/10.1002/ccd.31583.

32. A. Schaefer, M. Linder, M. Seiffert, et al., "Comparison of Latest Generation Transfemoral Self-Expandable and Balloon-Expandable Transcatheter Heart Valves," *Interactive CardioVascular and Thoracic Surgery* 25 (2017): 905–911, https://doi.org/10.1093/icvts/ivx194.

33. M. Arsalan and T. Walther, "Durability of Prostheses for Transcatheter Aortic Valve Implantation," *Nature Reviews Cardiology* 13 (2016): 360–367, https://doi.org/10.1038/nrcardio.2016.43.

34. J. Butany, C. Fayet, M. S. Ahluwalia, et al., "Biological Replacement Heart Valves," *Cardiovascular Pathology* 12 (2003): 119–139, https://doi.org/10.1016/S1054-8807(03)00002-4.

35. J. Liao and I. Vesely, "Skewness Angle of Interfibrillar Proteoglycans Increases With Applied Load on Mitral Valve Chordae Tendineae," *Journal of Biomechanics* 40 (2007): 390–398, https://doi.org/10.1016/j.jbiomech.2005.12.011.

36. M. Misfeld and H.-H. Sievers, "Heart Valve Macro- and Microstructure," *Philosophical Transactions of the Royal Society B: Biological Sciences* 362 (2007): 1421–1436, https://doi.org/10.1098/rstb.2007.2125.

37. S. Rigozzi, R. Müller, A. Stemmer, and J. G. Snedeker, "Tendon Glycosaminoglycan Proteoglycan Sidechains Promote Collagen Fibril Sliding—AFM Observations at the Nanoscale," *Journal of Biomechanics* 46, no. 4 (2013): 813–818, https://doi.org/10.1016/j.jbiomech.2012.11.017.

38. J. Tang, X. Chen, F. Liu, L. Zeng, Z. Suo, and J. Tang, "Why Are Soft Collagenous Tissues so Tough?," *Science Advances* 11 (2025): 0808, https://doi.org/10.1126/sciadv.adw0808.

39. S. L. Sellers, C. T. Turner, J. Sathananthan, et al., "Transcatheter Aortic Heart Valves," *JACC: CARDIOVASCULAR IMAGING* 12, no. 1 (2019), https://doi.org/10.1016/j.jcmg.2018.06.028.

40. C. Lee, H.-G. Lim, C.-H. Lee, and Y. Jin, "Effects of Glutaraldehyde Concentration and Fixation Time on Material Characteristics and Calcification of Bovine Pericardium: Implications for the Optimal Method of Fixation of Autologous Pericardium Used for Cardiovascular Surgery," *Interactive CardioVascular and Thoracic Surgery* 24 (2017): 402–406, https://doi.org/10.1093/icvts/ivw356.

41. Y. Yang, J. Zhang, F. Kong, et al., "A Robust Biprotein Stabilized Pericardium Valve Material Priming Resistance to Calcification," *ACS Applied Bio Materials* (2025), https://doi.org/10.1021/acsabm.5c00665.

42. B. Rahmani, C. McGregor, G. Byrne, and G. Burriesci, "A Durable Porcine Pericardial Surgical Bioprosthetic Heart Valve: A Proof of Concept," *Journal of Cardiovascular Translational Research* 12 (2019): 331–337, https://doi.org/10.1007/s12265-019-09868-3.

43. K. H. Yap, R. Murphy, M. Devbhandari, and R. Venkateswaran, "Aortic Valve Replacement: Is Porcine or Bovine Valve Better?," *Interactive CardioVascular and Thoracic Surgery* 16 (2013): 361–373, https://doi.org/10.1093/icvts/ivs447.

44. R. F. Siddiqui, J. R. Abraham, and J. Butany, "Bioprosthetic Heart Valves: Modes of Failure," *Histopathology* 55 (2009): 135–144, https://doi.org/10.1111/j.1365-2559.2008.03190.x.

45. S. Okutucu, A. Khan Niazi, D. Oliveira, S. Gorkem, and A. Oto, "A Systematic Review on Durability and Structural Valve Deterioration in TAVR and Surgical AVR," *Acta Cardiologica* 76, no. 9 (2021): 921–932, https://doi.org/10.1080/00015385.2020.1858250.

46. J. Soares, K. Risten R F Eaver, W. Hang, et al., "Biomechanical Behavior of Bioprosthetic Heart Valve Heterograft Tissues: Characterization, Simulation, and Performance," *Cardiovascular Engineering and Technology* 7, no. 4 (2016): 309–351, https://doi.org/10.1007/s13239-016-0276-8.

47. F. Oveissi, S. Na, A. Lee, D. S. Winlaw, and F. Dehghani, "Materials and Manufacturing Perspectives in Engineering Heart Valves: a Review," *Materials Today Bio* 5 (2020): 100038, https://doi.org/10.1016/j.mtbio.2019.100038.

48. A. Trimaille, A. Carmona, S. Hmadeh, and D. P. Truong, "Transcatheter Aortic Valve Durability: Focus on Structural Valve Deterioration," *Journal of the American Heart Association* (2025): 1–20, https://doi.org/10.1161/JAHA.125.041505.

49. I. Akin, S. Kische, T. C. Rehders, et al., "Indication for Percutaneous Aortic Valve Implantation," *Archives of Medical Science* 3, no. 3 (2010): 296–302, https://doi.org/10.5114/aoms.2010.14247.

50. A. Anselmi, E. Flécher, V. G. Ruggieri, et al., "Long-Term Results of the Medtronic Mosaic Porcine Bioprosthesis in the Aortic Position," *The Journal of Thoracic and Cardiovascular Surgery* (2014): 5–12, https://doi.org/10.1016/j.jtcvs.2013.07.005.

51. D. Capodanno, A. S. Petronio, B. Prendergast, et al., "Standardized Definitions of Structural Deterioration and Valve Failure in Assessing Long-Term Durability of Transcatheter and Surgical Aortic Bioprosthetic Valves: a Consensus Statement from the European Association of Percutaneous Cardiovascular Interve," *European Journal of Cardio-Thoracic Surgery* 52 (2017): 408–417, https://doi.org/10.1093/ejcts/ezx244.

52. L. H. Edmunds Jr., R. E. Clark, L. H. Cohn, G. L. Grunkemeier, D. C. Miller, and R. D. Weisel, "Guidelines for Reporting Morbidity and Mortality after Cardiac Valvular Operations," *European Journal of Cardio-Thoracic Surgery* 10 (1996): 812–816, https://doi.org/10.1016/S1010-7940(96)80347-2.

53. D. Dvir, T. Bourguignon, C. M. Otto, et al., "Standardized Definition of Structural Valve Degeneration for Surgical and Transcatheter Bioprosthetic Aortic Valves," *Circulation* (2018): 388–399, https://doi.org/10.1161/CIRCULATIONAHA.117.030729.

54. H. Baumgartner, J. Hung, J. Bermejo, et al., "Recommendations on the Echocardiographic Assessment of Aortic Valve Stenosis: a Focused Update from the European Association of Cardiovascular Imaging and the American Society of Echocardiography," *Journal of the American Society of Echocardiography* 30, no. 4 (2017): 372–392, https://doi.org/10.1016/j.echo.2017.02.009.

55. R. Manzo, F. Ilardi, D. Nappa, et al., "Echocardiographic Evaluation of Aortic Stenosis: a Comprehensive Review," *Diagnostics* 13, no. 15 (2023): 2527, https://doi.org/10.3390/diagnostics13152527.

56. J. L. Zamorano, L. P. Badano, C. Bruce, et al., "EAE/ASE Recommendations for the Use of Echocardiography in New Transcatheter

Interventions for Valvular Heart Disease," *European Heart Journal* 32, no. 17 (2011): 2189–2214, https://doi.org/10.1093/eurheartj/ehr259.

57. S. Shames, A. Koczo, R. Hahn, Z. Jin, M. H. Picard, and L. D. Gillam, "Flow Characteristics of the SAPIEN Aortic Valve: the Importance of Recognizing in-Stent Flow Acceleration for the Echocardiographic Assessment of Valve Function," *Journal of the American Society of Echocardiography* 25, no. 6 (2012): 603–609, https://doi.org/10.1016/j.echo.2012.02.013.

58. W. A. Zoghbi, J. B. Chambers, J. G. Dumesnil, et al., "Recommendations for Evaluation of Prosthetic Valves With Echocardiography and Doppler Ultrasound," *Journal of the American Society of Echocardiography* 22 (2009): 975–1014, https://doi.org/10.1016/j.echo.2009.07.013.

59. R. Rosenhek, T. Binder, G. Maurer, and H. Baumgartner, "Normal Values for Doppler Echocardiographic Assessment of Heart Valve Prostheses," *Journal of the American Society of Echocardiography* 16, no. 11 (2003): 1116–1127, https://doi.org/10.1067/S0894-7317(03)00638-2.

60. G. Pache, S. Schoechlin, P. Blanke, et al., "Early Hypo-Attenuated Leaflet Thickening in Balloon-Expandable Transcatheter Aortic Heart Valves," *European Heart Journal* 37 (2016): 2263–2271, https://doi.org/10.1093/eurheartj/ehv526.

61. H. N. Rashid, R. Rajani, J. Leipsic, et al., "Computed Tomography Imaging for Subclinical Lea Fl Et Thrombosis Following Surgical and Transcatheter Aortic Valve Replacement," *Journal of Cardiovascular Computed Tomography* 17 (2023): 2–10, https://doi.org/10.1016/j.jcct.2022.11.001.

62. J. Tambe, L. Mbuagbaw, G. Nguefack-Tsague, J. Foyet, and P. Ongolo-Zogo, "Multidetector Computed Tomography Utilization in an Urban Sub-Saharan Africa Setting: User Characteristics, Indications and Appropriateness," *Pan African Medical Journal* 37, no. 42 (2020), https://doi.org/10.11604/pamj.2020.37.42.21176.

63. Y. Zhang, Y. Wang, J. Hao, et al., "A Study on Comprehensive Anti - Calcification Treatment Technology for Bioprosthetic Valves," *Journal of Materials Science: Materials in Engineering* 20, no. 47 (2025), https://doi.org/10.1186/s40712-025-00263-2.

64. I. Vesely and A. Lozon, "Natural Preload of Aortic Valve Leaflet Components during Glutaraldehyde Fixation: Effects on Tissue Mechanics," *Journal of Biomechanics* 26, no. 2 (1993): 121–131, https://doi.org/10.1016/0021-9290(93)90043-E.

65. A. E. Kostyunin, T. V. Glushkova, T. N. Akentyeva, et al., "Enzymatic Degradation of Collagen as a Factor Enhancing Calcification of Epoxy-Treated Bioprosthetic Heart Valves: in Vitro Modeling Data," *Siberian Scientific Medical Journal* 2512, no. 3 (2025): 2410–2520, https://doi.org/10.18699/SSMJ20250313.

66. A. Koziarz, A. Makhdoum, J. Butany, M. Ouzounian, and J. Chung, "Modes of Bioprosthetic Valve Failure: a Narrative Review," *Current Opinion in Cardiology* 35, no. 2 (2020): 123–132, https://doi.org/10.1097/HCO.0000000000000711.

67. F. J. Schoen and R. J. Levy, "Calcification of Tissue Heart Valve Substitutes: Progress toward Understanding and Prevention," *The Annals of Thoracic Surgery* 79 (2005): 1072–1080, https://doi.org/10.1016/j.athoracsur.2004.06.033.

68. D. Vella, P. Boodagh, L. Modica, D. M. S. Ye, and F. Cosentino, "In Vitro Evaluation of Biomaterials for Heart Valve Prosthesis: High Hydrostatic and Enzymatic Treatments as Alternative for Bio-Derived Materials," *Journal of Biomedical Materials Research Part B: Applied Biomaterials* 113 (2025): 35592, https://doi.org/10.1002/jbm.b.35592.

69. D. T. Simionescu, "Prevention of Calcification in Bioprosthetic Heart Valves: Challenges and Perspectives," *Expert Opinion on Biological Therapy* 4, no. 12 (2004): 1971–1985, https://doi.org/10.1517/14712598.4.12.1971.

70. A. F. Badria, P. G. Koutsoukos, and D. Mavrilas, "Decellularized Tissue-Engineered Heart Valves Calci Fi Cation: What Do Animal and Clinical Studies Tell Us?," *Journal of Materials Science: Materials in Medicine* 31, no. 132 (2020), https://doi.org/10.1007/s10856-020-06462-x.

71. D. F. Williams, D. Bezuidenhout, J. D. Villiers, and P. Human, "Long-Term Stability and Biocompatibility of Pericardial Bioprosthetic Heart Valves," *Frontiers in Cardiovascular Medicine* 8 (2021): 1–17, https://doi.org/10.3389/fcvm.2021.728577.

72. M. D. Barbera, E. Pettenazzo, U. Livi, et al., "Structural Valve Deterioration and Mode of Failure of Stentless Bioprosthetic Valves," *Cardiovascular Pathology* 51 (2021): 107301, https://doi.org/10.1016/j.carpath.2020.107301.

73. S. Mohammadi, R. Baillot, P. Voisine, and P. Mathieu, "Structural Deterioration of the Freestyle Aortic Valve: Mode of Presentation and Mechanisms," *The Journal of Thoracic and Cardiovascular Surgery* 132, no. 2 (2005): 401–406, https://doi.org/10.1016/j.jtcvs.2006.03.056.

74. E. Tsolaki, P. Corso, R. Zboray, et al., "Multiscale Multimodal Characterization and Simulation of Structural Alterations in Failed Bioprosthetic Heart Valves," *Acta Biomaterialia* 169 (2023): 138–154, https://doi.org/10.1016/j.actbio.2023.07.044.

75. M. Sivaguru, S. Mori, K. W. Fouke, et al., "Osteopontin Stabilization and Collagen Containment Slows Amorphous Calcium Phosphate Transformation during Human Aortic Valve Leaflet Calcification," *Scientific Reports* 14 (2024): 12222, https://doi.org/10.1038/s41598-024-62962-8.

76. D. Annamalai, T. Ramamoorthy, A. M. Soloman, et al., "Combinatorial Glyoxal Cross-Linking and Glutamic Acid Capping for Mitigating Calcification in Bovine Pericardium," *Chemistry—An Asian Journal* 20, no. 19 (2025): 00652, https://doi.org/10.1002/asia.202500652.

77. X. Yu, J. Ding, Y. He, et al., "Porcine Pericardium Crosslinked With POSS-PEG-CHO Possesses Weakened Immunogenicity and Anti-Calcification Property," *Materials Today Bio* (2025), https://doi.org/10.1016/j.mtbio.2025.101677.

78. Z. Sun, J. Liu, X. Wang, et al., "Epoxy Chitosan-Crosslinked Acellular Bovine Pericardium With Improved Anti-Calci Fi Cation and Biological Properties," *ACS Applied Bio Materials* 3 (2020): 2275, https://doi.org/10.1021/acsabm.0c00067.

79. H. Pu, T. Yu, C. Wang, et al., "Novel Non-Glutaraldehyde bioprosthetic Heart Valve Construction Strategy Based on ATRP With Enhanced Anticoagulant and Anti-Calcification properties," *Journal of Materials Chemistry B* 13 (2025): 5643–5654, https://doi.org/10.1039/D4TB02800G.

80. J. Chen, S. Li, X. Chen, et al., "M2 Macrophage-Derived Exosome-Modified Bioprosthetic Heart Valves With Enhanced Anti-Inflammatory, Anticoagulant and Anticalcification Properties," *Materials & Design* 254 (2025): 114018, https://doi.org/10.1016/j.matdes.2025.114018.

81. S. Shi, X. Wei, X. Peng, X. Pu, and S. Feng, "An Oxidized Chondroitin Sulfate-Crosslinked and CuCDs-Loaded Decellularized Bovine Pericardium With Improved Anti-Coagulation, Pro-Endothelialization and Anti-Calcification Properties for BHVs," *Journal of Materials Chemistry B* 13 (2025): 7196–7212, https://doi.org/10.1039/d5tb00827a.

82. A. Mastrofini, M. Marino, E. Karlöf, U. Hedin, and T. Christian Gasser, "On the Impact of Residual Strains in the Stress Analysis of Patient-Specific Atherosclerotic Carotid Vessels: Predictions Based on the Homogenous Stress Hypothesis," *Annals of Biomedical Engineering* 52, no. 5 (2024): 1347–1358, https://doi.org/10.1007/s10439-024-03458-4.

83. F. Kong, J. Zhang, Y. Yang, Y. Zhang, J. Ge, and J. Song, "A Novel Aldehyde Scavenging Modification Boosted Pericardium Valve Materials against Calcification," *Advanced Healthcare Materials* 1–13 (2025): 2500856, https://doi.org/10.1002/adhm.202500856.

84. K. Li, Q. Hu, L. Wang, et al., "Engineering of Bioprosthetic Heart Valves With Synergistic Zwitterionic Surface Modification and Zirconium Cross—Linking for Improved Biocompatibility and Durability," *Acta Biomaterialia* 201 (2025): 266–282, https://doi.org/10.1016/j.actbio.2025.06.010.

85. Y. Yang, L. Lan, and Y. Lin, "Mechanistic Insights into Bioprosthetic Heart Valve Calcification and Anti-Calcification Strategies," *Reviews in Cardiovascular Medicine* 26, no. 5 (2025), https://doi.org/10.31083/RCM36688.

86. X. Huang, B. Wei, L. Chen, L. Yang, C. Zheng, and Y. Wang, "Degeneration Mechanisms and Advancements in Optimization for Preparation and Crosslinking Strategy of Pericardium-Based Bioprosthetic Heart Valves," *Acta Biomaterialia* 201 (2025): 51–74, https://doi.org/10.1016/j.actbio.2025.05.062.

87. T. Theodoropoulou, I. Mourouzis, A. Katsaouni, C. Pantos, K. Tsioufis, and K. Toutouzas, "Valvular Interstitial Cells as a Novel Therapeutic Target for Preventing Calcific Aortic Valve Disease," *European Journal of Pharmacology* 1003 (2025): 177985, https://doi.org/10.1016/j.ejphar.2025.177985.

88. N. Kiesendahl, C. Schmitz, M. Menne, T. Schmitz-Rode, and U. Steinseifer, "In Vitro Calcification of Bioprosthetic Heart Valves: Investigation of Test Fluids," *Annals of Biomedical Engineering* 48, no. 1 (2020): 282–297, https://doi.org/10.1007/s10439-019-02347-5.

89. N. Kiesendahl, C. Schmitz, M. Menne, and T. Schmitz-Rode, "In Vitro Calcification of Bioprosthetic Heart Valves: Test Fluid Validation on Prosthetic Material Samples," *Annals* 49, no. 2 (2021): 885–899, https://doi.org/10.1007/s10439-020-02618-6.

90. N. Kiesendahl, C. Schmitz, L. Peters, and J. C. Clauser, "In Vitro Calcification of Bioprosthetic Heart Valves: Method Validation by Comparative Heart Valve Calcification Testing," *Artificial Organs* (2025): 1–10, https://doi.org/10.1111/aor.70015.

91. S. R. Rickaby and N. H. Scott, "A Cyclic Stress Softening Model for the Mullins Effect," *International Journal of Solids and Structures* 50, no. 1 (2013): 111–120, https://doi.org/10.1016/j.ijsolstr.2012.09.006.

92. A. Whelan, E. Williams, E. Fitzpatrick, et al., "Collagen Fibre-Me Diate D Mechanical Damage Increases Calcification of Bovine Pericardium for Use in Bioprosthetic Heart Valves," *Acta Biomaterialia* 128 (2021): 384–392, https://doi.org/10.1016/j.actbio.2021.04.046.

93. S. Chen, Y. Wang, L. Yang, et al., "Biodegradable Elastomers for Biomedical Applications," *Progress in Polymer Science* 147 (2023): 101763, https://doi.org/10.1016/j.progpolymsci.2023.101763.

94. T. C. Gasser, "An Irreversible Constitutive Model for Fibrous Soft Biological Tissue: a 3-D Microfiber Approach With Demonstrative Application to Abdominal Aortic Aneurysms," *Acta Biomaterialia* 7, no. 6 (2011): 2457–2466, https://doi.org/10.1016/j.actbio.2011.02.015.

95. M. Marino, "Molecular and Intermolecular Effects in Collagen Fibril Mechanics: a Multiscale Analytical Model Compared With Atomistic and Experimental Studies," *Biomechanics and Modeling in Mechanobiology* 15, no. 1 (2016): 133–154, https://doi.org/10.1007/s10237-015-0707-8.

96. M. Marino, "Constitutive Modeling of Soft Tissues," in *Encyclopedia of Biomedical Engineering*, ed. R Narayan, (Elsevier, 2019), 81–110, https://doi.org/10.1016/B978-0-12-801238-3.99926-4.

97. F. Shojaeianforoud, L. Marin, W. J. Anderl, M. Marino, B. Coats, and K. L. Monson, "Repeated Loading and Damage Progression in Cerebral Arteries," *Acta Biomaterialia* 197 (2025): 256–265, https://doi.org/10.1016/j.actbio.2025.03.027.

98. A. J. Dalgliesh, M. Parvizi, C. Noble, and L. G. G. Id, "Effect of Cyclic Deformation on Xenogeneic Heart Valve Biomaterials," *PLoS ONE* 14 (2019): 1–21.

99. L. Musumeci, N. Jacques, A. Hego, A. Nchimi, P. Lancellotti, and C. Oury, "Prosthetic Aortic Valves: Challenges and Solutions," *Frontiers in Cardiovascular Medicine* 5 (2018): 1–5, https://doi.org/10.3389/fcvm.2018.00046.

100. H. Li, S. Li, Y. Lei, et al., "Advancements and Perspectives in the Bioprosthetic Heart Valve: a Comprehensive Review on Biomaterial," *Journal of the American Heart Association* 14 (2025): 1–19, https://doi.org/10.1161/JAHA.125.043061.

101. J. Wang, J. Sun, J. Chen, et al., "Self-Assembled Entanglements in Elastomers for Superior Toughness and Fatigue Resistance," *Macromolecules* 58 (2025): 4438–4446, https://doi.org/10.1021/acs.macromol.5c00531.

102. H. He, X. Zhou, Y. Lai, et al., "Chain Entanglement Enhanced Strong and Tough Wool Keratin /Albumin Fibers for Bioabsorbable and Immunocompatible Surgical Sutures," *Nature Communications* 16 (2025): 3004, https://doi.org/10.1038/s41467-025-58171-0.

103. M. D. Hager, P. Greil, C. Leyens, S. V. D. Zwaag, and U. S. Schuber, "Self-Healing Materials.Pdf," *Advanced Materials* 22, no. 47 (2010): 5424–5430.

104. Y. Wang, X. Huang, and X. Zhang, "Ultrarobust, Tough and Highly Stretchable Self-Healing Materials Based on Cartilage-Inspired Noncovalent Assembly Nanostructure," *Nature Communications* 12 (2021): 1291, https://doi.org/10.1038/s41467-021-21577-7.

105. Z. Wei, H. Ye, Y. Li, X. Li, Y. Liu, and Y. Chen, "Mechanically Tough, Adhesive, Self-Healing Hydrogel Promotes Annulus Fibrosus Repair via Autologous Cell Recruitment and Microenvironment Regulation," *Acta Biomaterialia* 178 (2024): 50–67, https://doi.org/10.1016/j.actbio.2024.02.020.

106. B. Cwalina, A. Turek, J. Nozynski, M. Jastrzebska, and Z. Nawrat, "Structural Changes in Pericardium Tissue Modified With Tannic Acid," *The International Journal of Artificial Organs* 28, no. 6 (2005): 648–653, https://doi.org/10.1177/039139880502800614.

107. M. Jastrzebska, J. Zalewska-Rejdak, R. Wrzalik, et al., "Tannic Acid-Stabilized Pericardium Tissue: IR Spectroscopy, Atomic Force Microscopy, and Dielectric Spectroscopy Investigations," *Journal of Biomedical Materials Research Part A* 78A (2006): 148–156, https://doi.org/10.1002/jbm.a.30717.

108. M. Jastrzebska, R. Wrzalik, A. Kocot, J. Zalewska-Rejdak, and B. Cwalina, "Hydration of Glutaraldehyde-Fixed Pericardium Tissue: Raman Spectroscopic Study," *Journal of Raman Spectroscopy* 34 (2003): 424–431, https://doi.org/10.1002/jrs.1016.

109. A. Whelan, E. Williams, D. R. Nolan, et al., "Bovine Pericardium of High Fibre Dispersion Has High Fatigue Life and Increased Collagen Content; Potentially an Untapped Source of Heart Valve Leaflet Tissue," *Annals of Biomedical Engineering* 49, no. 3 (2021): 1022–1032, https://doi.org/10.1007/s10439-020-02644-4.

110. N. Sadat, A. Osterloh, M. Scharfschwerdt, and S. Ensminger, "Durability Testing With Calcification of Surgical Aortic Valves and Transcatheter Heart Valves: an in Vitro Study," *Interdisciplinary Cardio-Vascular and Thoracic Surgery* 40, no. 9 (2025): ivaf196, https://doi.org/10.1093/icvts/ivaf196.2.

111. Q. Tong, J. Cai, Z. Wang, et al., "Recent Advances in the Modification and Improvement of Bioprosthetic Heart Valves," *Small* 20 (2024): 2309844, https://doi.org/10.1002/smll.202309844.

112. G. Campion, K. Hershberger, A. Whelan, J. Conroy, and C. Lally, "A Biomechanical and Microstructural Analysis of Bovine and Porcine Pericardium for Use in Bioprosthetic Heart Valves," *Structural Heart* 5, no. 5 (2021): 486–496, https://doi.org/10.1080/24748706.2021.1938317.

113. D. Jin, S. Yang, S. Wu, M. Yin, and H. Kuang, "A Functional PVA Aerogel-Based Membrane Obtaining Sutureability through Modified Electrospinning Technology and Achieving Promising Anti-Adhesion Effect after Cardiac Surgery," *Bioactive Materials* 10 (2022): 355–366, https://doi.org/10.1016/j.bioactmat.2021.08.013.

114. M. Ra, B. Ekser, M. Ah, and C. Dkc, "Bioprosthetic Heart Valves of the Future," *Xenotransplantation* 21 (2014): 1–10, https://doi.org/10.1111/xen.12080.

115. M. Jastrzebska and B. Barwinski, "Atomic Force Microscopy Investigation of Chemically Stabilized Pericardium Tissue," *European Physical Journal E* 388 (2005): 381, https://doi.org/10.1140/epje/i2004-10093-1.

116. F. Nudelman, G. De With, and N. A. J. M. Sommerdijk, "Cryo-Electron Tomography: 3-Dimensional Imaging of Soft Matter," *Soft Matter* (2011): 17–24, https://doi.org/10.1039/c0sm00441c.

117. M. J. Buehler, "A Computational Building Block Approach towards Multiscale Architected Materials Analysis and Design With Application to Hierarchical Metal Metamaterials," *Modelling and Simulation in*

Materials Science and Engineering 31, no. 5 (2023): 054001, https://doi.org/10.1088/1361-651X/accfb5.

118. A. J. Lew, J. Kai, and M. J. Buehler, "Designing Architected Materials for Mechanical Compression via Simulation, Deep Learning, and Experimentation," *Npj Computational Materials* 9, no. 1 (2023), https://doi.org/10.1038/s41524-023-01036-1.

119. Y. Liu, B. Song, J. Zhang, C. Gaidau, and H. Gu, "Aluminum Tanning of Hide Powder and Skin Pieces under Microwave Irradiation," *Journal of Leather Science and Engineering* 2, no. 23 (2020), https://doi.org/10.1186/s42825-020-00037-w.

120. K. Pietrucha and M. Safandowska, "Dialdehyde Cellulose-Crosslinked Collagen and Its Physicochemical Properties," *Process Biochemistry* 50, no. 12 (2015): 2105–2111, https://doi.org/10.1016/j.procbio.2015.09.025.

121. M. J. Jafari, F. G. Bäcklund, T. Arndt, et al., "Force-Induced Structural Changes in Spider Silk Fibers Introduced by ATR-FTIR Spectroscopy," *ACS Applied Polymer Materials* 5, no. 11 (2023): 9433–9444, https://doi.org/10.1021/acsapm.3c01892.

122. M. Rubinstein and R. H. Colby, "Polymer Physics," in *Polymer Physics Applications to Molecular Association and Thermoreversible Gelation* (Oxford University, 2003), https://doi.org/10.1017/CBO9780511975691.

123. G. M. Fomovsky, S. Thomopoulos, and J. W. Holmes, "Contribution of Extracellular Matrix to the Mechanical Properties of the Heart," *Journal of Molecular and Cellular Cardiology* 48, no. 3 (2010): 490–496, https://doi.org/10.1016/j.yjmcc.2009.08.003.

124. P. Boodagh, L. Modica De Mohac, Y. Hayashi, et al., "Photooxidation Cross-Linked Glutaraldehyde Cross-Linked or Enzyme and Hydrostatic," *Journal of Biomedical Materials Research Part B: Applied Biomaterials* 113 (2025): 35529, https://doi.org/10.1002/jbm.b.35529.

125. R. T. Gaul, D. R Nolan, and C. Lally, "Collagen Fibre Characterisation in Arterial Tissue under Load Using SALS," *Journal of the Mechanical Behavior of Biomedical Materials* 75 (2017): 359–368, https://doi.org/10.1016/j.jmbbm.2017.07.036.

126. A. Whelan, J. Duffy, R. T. Gaul, et al., "Collagen Fibre Orientation and Dispersion Govern Ultimate Tensile Strength, Stiffness and the Fatigue Performance of Bovine Pericardium," *Journal of the Mechanical Behavior of Biomedical Materials* 90 (2019): 54–60, https://doi.org/10.1016/j.jmbbm.2018.09.038.

127. B. D. Quan and E. D. Sone, "Cryo-TEM Analysis of Collagen Fibrillar Structure," in *Research Methods in BIomineralization Science*, 1st ed. (Elsevier Inc, 2013), https://doi.org/10.1016/B978-0-12-416617-2.00009-6.

128. P. Echlin, *Handbook of Sample Preparation for Scanning Electron Microscopy and X-Ray Microanalysis*, (Springer, 2009), https://doi.org/10.1007/978-0-387-85731-2.

129. J. Liu, S. Zhong, H. Lan, et al., "Mapping the Calcification of Bovine Pericardium in Rat Model by Enhanced Micro-Computed Tomography," *Biomaterials* 35, no. 29 (2014): 8305–8311, https://doi.org/10.1016/j.biomaterials.2014.06.026.

130. S. Yousefi, H. Borna, A. Rohani, C. Wen, and A. Nouri, "Surface Modification of Mechanical Heart Valves: a Review," *European Polymer Journal* 205 (2024): 112726, https://doi.org/10.1016/j.eurpolymj.2023.112726.

131. N. David and K. Petr, "Gwyddion: An open-source software for SPM data analysis," *Central European Journal of Physics* 10, no. 1 (2012) 181–188.

132. H. E. Burton and D. M. Espino, "The Effect of Mechanical Overloading on Surface Roughness of the Coronary Arteries," *Hindawi Applied Bionics and Biomechanics* 7 (2019): 2784172, https://doi.org/10.1155/2019/2784172.

133. P. Boloori Zadeh, S. C. Corbett, and H. Nayeb-hashemi, "Effects of Fluid Flow Shear Rate and Surface Roughness on the Calcification of Polymeric Heart Valve Leaflet," *Materials Science & Engineering C* 33, no. 5 (2013): 2770–2775, https://doi.org/10.1016/j.msec.2013.02.042.

134. Z. Yin, C. Armour, H. Kandail, D. P. O. Regan, and T. Bahrami, "The Impact of Coronary Outflow and non-Newtonian Fluid Property on Aortic Valve Haemodynamics," *Biomechanics and Modeling in Mechanobiology* 24 (2025): 1401–1416, https://doi.org/10.1007/s10237-025-01975-2.

135. I. H. Jaffer, J. C. Fredenburgh, J. Hirsh, and J. I. Weitz, "Medical Device-Induced Thrombosis: What Causes It and How Can We Prevent It?," *Journal of Thrombosis and Haemostasis* 13 (2015): S72–S81, https://doi.org/10.1111/jth.12961.

136. J. H. Lee and H. B. Lee, "Platelet Adhesion onto Wettability Gradient Surfaces in the Absence and Presence of Plasma Proteins," *Journal of Biomedical Materials Research* 41, no. 2 (1998): 304–311, https://doi.org/10.1002/(SICI)1097-4636(199808)41:2⟨304::AID-JBM16⟩3.0.CO;2-K.

137. N. Yayapour and H. Nygren, "Interactions between Whole Blood and Hydrophilic or Hydrophobic Glass Surfaces: Kinetics of Cell Adhesion," *Colloids and Surfaces B: Biointerfaces* 15 (1999): 127–138, https://doi.org/10.1016/S0927-7765(99)00049-1.

138. J. Kuchinka, C. Willems, and D. V. Telyshev, "Control of Blood Coagulation by Hemocompatible Material Surfaces—A Review," *Bioengineering* 8, no. 12 (2021): 1–26, https://doi.org/10.3390/bioengineering8120215.

139. N. Recek, "Biocompatibility of Plasma-Treated Polymeric Implants," *Materials* 12, no. 2 (2019): 240, https://doi.org/10.3390/ma12020240.

140. A. C. Fischer-Cripps, *Nanoindentation* (Springer, 2011), https://doi.org/10.1007/978-1-4757-5943-3_4.

141. R. Das, A. Kumar, A. Patel, S. Vijay, S. Saurabh, and N. Kumar, "Biomechanical Characterization of Spider Webs," *Journal of the Mechanical Behavior of Biomedical Materials* 67 (2017): 101–109, https://doi.org/10.1016/j.jmbbm.2016.12.008.

142. G. Greco, J. Wolff, and N. M. Pugno, "Strong and Tough Silk for Resilient Attachment Discs: the Mechanical Properties of Piriform Silk, in the Spider Cupiennius Salei (Keyserling, 1877)," *Frontiers in Materials* 7, no. 138 (2020), https://doi.org/10.3389/fmats.2020.00138.

143. Y. Politi, M. Priewasser, E. Pippel, et al., "A Spider's Fang: How to Design an Injection Needle Using Chitin-Based Composite Material," *Advanced Functional Materials* 22, no. 12 (2012): 2519–2528, https://doi.org/10.1002/adfm.201200063.

144. S. Residori, G. Greco, and N. M. Pugno, "The Mechanical Characterization of the Legs, Fangs, and Prosoma in the Spider Harpactira Curvipes (Pocock 1897)," *Scientific Reports* 12, no. 1 (2022): 1–11, https://doi.org/10.1038/s41598-022-16307-y.

145. F. Tramacere, A. Kovalev, T. Kleinteich, S. N. Gorb, and B. Mazzolai, "Structure and Mechanical Properties of Octopus Vulgaris Suckers," *Journal of The Royal Society Interface* 11, no. 91 (2013): 20130816, https://doi.org/10.1098/rsif.2013.0816.

146. R. M. Cahalane and M. T. Walsh, "Nanoindentation of Calcified and Non-Calcified Components of Atherosclerotic Tissues," *Experimental Mechanics* 61 (2021): 67–80, https://doi.org/10.1007/s11340-020-00635-z.

147. A. Hemmasizadeh, M. Autieri, and K. Darvish, "Multilayer Material Properties of Aorta Determined from Nanoindentation Tests," *Journal of the Mechanical Behavior of Biomedical Materials* 15 (2012): 199–207, https://doi.org/10.1016/j.jmbbm.2012.06.008.

148. J. P. Meekel, G. Mattei, V. S. Costache, R. Balm, J. D. Blankensteijn, and K. K. Yeung, "A Multilayer Micromechanical Elastic Modulus Measuring Method in Ex Vivo Human Aneurysmal Abdominal Aortas," *Acta Biomaterialia* 96 (2019): 345–353, https://doi.org/10.1016/j.actbio.2019.07.019.

149. H. Hertz, "Über die Berührung Fester ElastischerKorper," *Journal Für Die Reine Und Angewandte Mathematik* 92 (1881): 156–171.

150. C. Zhang, Y. Li, L. Yang, and H. Zhao, "Dynamic Indentation and Microstructural Analysis of Artery under Pre-Strain in Different Directions," *Materials Today Communications* 42 (2025): 111041, https://doi.org/10.1016/j.mtcomm.2024.111041.

151. A. Tobaruela, F. J. Rojo, J. M. G. Paez, et al., "Indentation Hardness: a Simple Test That Correlates With the Dissipated-Energy Predictor for

Fatigue-Life in Bovine Pericardium Membranes for Bioprosthetic Heart Valves," *Journal of the Mechanical Behavior of Biomedical Materials* 61 (2016): 55–61, https://doi.org/10.1016/j.jmbbm.2016.01.010.

152. X. Deng, A. Hasan, S. Elsharkawy, et al., "Topographically Guided Hierarchical Mineralization," *Materials Today Bio* 11 (2021): 100119, https://doi.org/10.1016/j.mtbio.2021.100119.

153. L. V. Huckaby, R. N. Fortunato, L. V. Emerel, et al., "Wall Tensile Stress Maps of Human Aneurysmal Aorta Demonstrate a High Biaxiality Ratio Corresponds With Wall Tissue Microstructure and Local Oxidative Stress Response Distinctly for Bicuspid and Tricuspid Aortic Valve Patients," *Annals of Biomedical Engineering* 53 (2025): 2223–2238, https://doi.org/10.1007/s10439-025-03771-6.

154. K. Karatolios, A. Wittek, T. H. Nwe, et al., "Method for Aortic Wall Strain Measurement With Three-Dimensional Ultrasound Speckle Tracking and Fitted Finite Element Analysis," *The Annals of Thoracic Surgery* 96, no. 5 (2013): 1664–1671, https://doi.org/10.1016/j.athoracsur.2013.06.037.

155. T. A. Krouskop, D. Ph, D. R. Dougherty, F. S. Vinson, and D. Ph, "A Pulsed Doppler Ultrasonic System for Making Noninvasive Measurements of the Mechanical Properties of Soft Tissue," *Journal of Rehabilitation Research and Development* 24, no. 2 (1987): 1–8.

156. R. Akhtar, M. J. Sherratt, J. Kennedy Cruickshank, and B. Derby, "Characterizing the Elastic Properties of Tissues," *Materials Today* 14, no. 3 (2011): 96–105, https://doi.org/10.1016/S1369-7021(11)70059-1.

157. L. P. Argani, D. Misseroni, A. Piccolroaz, Z. Vinco, and D. Capuani, "Plastically-Driven variation of Elastic Stiffness in Green Bodies during Powder Compaction: Part I. Experiments and Elastoplastic Coupling," *Journal of the European Ceramic Society* 36 (2016): 2159–2167, https://doi.org/10.1016/j.jeurceramsoc.2016.02.012.

158. K. W. Nowak, M. Markowski, and T. Daszkiewicz, "Ultrasonic Determination of Mechanical Properties of Meat Products," *Journal of Food Engineering* 147 (2015): 49–55, https://doi.org/10.1016/j.jfoodeng.2014.09.024.

159. M. Pithioux, P. Lasaygues, and P. Chabrand, "An Alternative Ultrasonic Method for Measuring the Elastic Properties of Cortical Bone," *Journal of Biomechanics* 35 (2002): 961–968, https://doi.org/10.1016/S0021-9290(02)00027-1.

160. X. Guo, R. Lin, K. Zhang, H. Zhang, N. Zhang, and G. Song, "Biomimetic Multilayered Polymeric Heart Valve Featuring Ultra-Thin Thickness and Exceptional Durability," *Biochemical and Biophysical Research Communications* 756 (2025): 151609, https://doi.org/10.1016/j.bbrc.2025.151609.

161. H. Zhou, L. Wu, and Q. Wu, "Structural Stability of Novel Composite Heart Valve Prostheses—Fatigue and Wear Performance," *Biomedicine & Pharmacotherapy* 136 (2021): 111288, https://doi.org/10.1016/j.biopha.2021.111288.

162. J. M. Mansour, D.-W. M. Gu, C.-Y. Chung, et al., "Towards the Feasibility of Using Ultrasound to Determine Mechanical Properties of Tissues in a Bioreactor," *Annals of Biomedical Engineering* 42, no. 10 (2014): 2190–2202, https://doi.org/10.1007/s10439-014-1079-4.

163. M. Alloisio, A. Siika, D. Freiholtz, et al., "Fracture Properties of Porcine versus Human Thoracic Aortas from Tricuspid /Bicuspid Aortic Valve Patients via Symmetry-Constraint Compact Tension Testing," *Scientific Reports* 15, no. 667 (2025): 1–12, https://doi.org/10.1038/s41598-024-83233-6.

164. T. Pham, F. Sulejmani, E. Shin, W. Di, and W. Sun, "Quantification and Comparison of the Mechanical Properties of Four Human Cardiac Valves," *Acta Biomaterialia* 54 (2017): 345–355, https://doi.org/10.1016/j.actbio.2017.03.026.

165. R. Gauvin, G. Marinov, Y. Mehri, et al., "A Comparative Study of Bovine and Porcine Pericardium to Highlight Their Potential Advantages to Manufacture Percutaneous Cardiovascular Implants," *Journal of Biomaterials Applications* 28, no. 4 (2012): 552–565, https://doi.org/10.1177/0885328212465482.

166. A. Caballero, F. Sulejmani, C. Martin, T. Pham, and W. Sun, "Evaluation of Transcatheter Heart Valve Biomaterials: Biomechanical Characterization of Bovine and Porcine Pericardium," *Journal of the Mechanical Behavior of Biomedical Materials* 75 (2017): 486–494, https://doi.org/10.1016/j.jmbbm.2017.08.013.

167. D. Arbeiter, N. Grabow, Y. Wessarges, K. Sternberg, and K. Schmitz, "Suitability of Porcine Pericardial Tissue for Heart Valve Engineering: Biomechanical Properties," *Biomedical Engineering / Biomedizinische Technik* 57 (2012): 882–883, https://doi.org/10.1515/bmt-2012-4332.

168. G. Greco, B. Schmuck, S. K. Jalali, N. M. Pugno, and A. Rising, "Influence of Experimental Methods on the Mechanical Properties of Silk Fibers: a Systematic Literature Review and Future Road Map," *Biophysics Reviews* 4 (2023): 031301, https://doi.org/10.1063/5.0155552.

169. J. M. Lee and D. R. Boughner, "Mechanical Properties of human Pericardium. Differences in Viscoelastic Response When Compared With Canine Pericardium," *Circulation Research* 57, no. 3 (1985): 475–481, https://doi.org/10.1161/01.RES.57.3.475.

170. J. Zhao, A. Bahatibieke, G. Liu, et al., "Dynamically Reshaping High Density Hydrogen Bonds Enhanced Polyurethane Used as Artificial Heart Valves With Enhanced Fatigue Resistance, Anti-Calcification and Blood Compatibility," *Chemical Engineering Journal* 502 (2024): 158015, https://doi.org/10.1016/j.cej.2024.158015.

171. Y. Zhang, H. Wang, Y. Zhong, W. Wang, Z. Zhang, and Q. He, "A Study on the Correlation between Calcific Aortic Valve Disease and Carotid Artery Elasticity," *Reviews in Cardiovascular Medicine* 26, no. 5 (2025): 1–8, https://doi.org/10.31083/RCM26821.

172. J. A. Stella and M. S. Sacks, "On the Biaxial Mechanical Properties of the Layers of the Aortic Valve Leaflet," *Journal of Biomechanical Engineering* 129 (2007): 757–766, https://doi.org/10.1115/1.2768111.

173. X. Hu, Z. He, and H. Wang, "Effects of a Drying Treatment on the Mechanical Properties and Hemodynamic Characteristics of Bovine Pericardial Bioprosthetic Valves," *Journal of Functional Biomaterials* 16, no. 12 (2025): 1–14, https://doi.org/10.3390/jfb16120434.

174. F. Q. Pancheri, R. A. Peattie, W. Lin, T. D. Ouellette, M. D. Iafrati, and A. Luis Dorfmann, "Histology and Biaxial Mechanical Behavior of Abdominal Aortic Aneurysm Tissue Samples," *Journal of Biomechanical Engineering* 139 (2017): 1–12, https://doi.org/10.1115/1.4035261.

175. P. Zioupos and J. C. Barbenel, "Mechanics of Native Bovine Pericardium," *Biomaterials* 15, no. 5 (1994): 366–373, https://doi.org/10.1016/0142-9612(94)90249-6.

176. D. Oswal, S. Korossis, S. Mirsadraee, et al., "Biomechanical Characterization of Decellularized and Cross-Linked Bovine Pericardium," *Journal of Heart Valve Disease* 16, no. 2 (2007): 165.

177. P. R. Umashankar, A. Sabareeswaran, and S. J. Shenoy, "Long-Term Healing of Mildly Cross-Linked Decellularized Bovine Pericardial Aortic Patch," *Journal of Biomedical Materials Research Part B: Applied Biomaterials* 105, no. 7 (2017): 2145–2152, https://doi.org/10.1002/jbm.b.33755.

178. A. Jannasch, J. Rix, C. Welzel, G. Schackert, M. Kirsch, and K. Ulla, "Brillouin Confocal Microscopy to Determine Biomechanical Properties of SULEEI-Treated Bovine Pericardium for Application in Cardiac Surgery," *Clinical Hemorheology and Microcirculation* 79 (2021): 179–192, https://doi.org/10.3233/CH-219119.

179. E. Filova, M. Steinerova, M. Travnickova, J. Knitlova, and J. Musilkova, "Accelerated in Vitro Recellularization of Decellularized Porcine Pericardium for Cardiovascular Grafts Accelerated in Vitro Recellularization of Decellularized Porcine Pericardium for Cardiovascular Grafts," *Biomedical Materials* 16 (2016): 025024, https://doi.org/10.1088/1748-605X/abbdbd.

180. S. Heyden, A. Nagler, C. Bertoglio, et al., "Material Modeling of Cardiac Valve Tissue: Experiments, Constitutive Analysis and Numerical Investigation," *Journal of Biomechanics* 48, no. 16 (2015): 4287–4296, https://doi.org/10.1016/j.jbiomech.2015.10.043.

181. R. Claramunt, J. María, G. Páez, L. Alvarez, A. Ros, and M. Concepción, "Fatigue Behaviour of Young Ostrich Pericardium," *Materials Science and Engineering: C* 32, no. 6 (2012): 1415–1420, https://doi.org/10.1016/j.msec.2012.04.020.

182. R. Claramunt, J. M. García Páez, L. Alvarez, J. Spottorno, A. Ros, and M. C. Casado, "Short-Term Fatigue Testing Can Predict Medium-Term Pericardium Behaviour," *Journal of the Mechanical Behavior of Biomedical Materials* 4, no. 8 (2011): 1929–1935, https://doi.org/10.1016/j.jmbbm.2011.06.009.

183. J. M. G. Paez, A. Carrera Sanmartın, E. Jorge Herrero, et al., "Durability of a Cardiac Valve Leaflet Made of Calf Pericardium: Fatigue and Energy Consumption," *Journal of Biomedical Materials Research Part A* 77A (2006): 839–849, https://doi.org/10.1002/jbm.a.

184. N. Pearson, G. M. Boiczyk, W. J. Anderl, M. Marino, S. Michael Yu, and K. L. Monson, "Softening of Elastic and Viscoelastic Properties Is Independent of Overstretch Rate in Cerebral Arteries," *Journal of the Mechanical Behavior of Biomedical Materials* 166 (2025): 106957, https://doi.org/10.1016/j.jmbbm.2025.106957.

185. M. Abbasi and A. N. Azadani, "Stress Analysis of Transcatheter Aortic Valve Leaflets under Dynamic Loading: Effect of Reduced Tissue Thickness," *Journal of Heart Valve Disease* 27, no. 4 (2017): 386–396.

186. A. A. E. Y. Kostyunin, M. A. Rezvova, E. A. Ovcharenko, T. V. Glushkova, and A. G. Kutikhin, "Degeneration of Bioprosthetic Heart Valves: Update 2020," *Journal of the American Heart Association* 9, no. 19 (2020): 018506, https://doi.org/10.1161/JAHA.120.018506.

187. C. J. Arthurs, R. Khlebnikov, A. Melville, et al., "CRIMSON: an Open-Source Software Framework for Cardiovascular Integrated Modelling and Simulation," *PLoS Computational Biology* (2021): 1–21, https://doi.org/10.1371/journal.pcbi.1008881.

188. F. Auricchio, M. Conti, S. Marconi, A. Reali, J. L. Tolenaar, and S. Trimarchi, "Patient-Specific Aortic Endografting Simulation: from Diagnosis to Prediction," *Computers in Biology and Medicine* 43, no. 4 (2013): 386–394, https://doi.org/10.1016/j.compbiomed.2013.01.006.

189. A. G. Kuchumov, A. Makashova, S. Vladimirov, V. Borodin, and A. Dokuchaeva, "Fluid—Structure Interaction Aortic Valve Surgery Simulation: a Review," *Fluids* 8 (2023): 295, https://doi.org/10.3390/fluids8110295.

190. A. Updegrove, N. Ilson, J. Merkow, H. Lan, A. L. Marsden, and S. C. Shadden, "SimVascular: an Open Source Pipeline for Cardiovascular Simulation," *Annals of Biomedical Engineering* 45, no. 3 (2017): 525–541, https://doi.org/10.1007/s10439-016-1762-8.

191. J. A. Brown, J. H. Lee, M. A. Smith, et al., "Patient–Specific Immersed Finite Element–Difference Model of Transcatheter Aortic Valve Replacement," *Annals of Biomedical Engineering* 51, no. 1 (2023): 103–116, https://doi.org/10.1007/s10439-022-03047-3.

192. K. Murdock, C. Martin, and W. Sun, "Characterization of Mechanical Properties of Pericardium Tissue Using Planar Biaxial Tension and Flexural Deformation," *Journal of the Mechanical Behavior of Biomedical Materials* 77 (2018): 148–156, https://doi.org/10.1016/j.jmbbm.2017.08.039.

193. A. Finotello, R. Gorla, N. Brambilla, F. Bedogni, F. Auricchio, and S. Morganti, "Finite Element Analysis of Transcatheter Aortic Valve Implantation: Insights on the Modelling of Self-Expandable devices," *Journal of the Mechanical Behavior of Biomedical Materials* 123 (2021): 104772, https://doi.org/10.1016/j.jmbbm.2021.104772.

194. A. Finotello, S. Morganti, and F. Auricchio, "Finite Element Analysis of TAVI: Impact of Native Aortic Root Computational Modeling Strategies on Simulation Outcomes," *Medical Engineering & Physics* 47 (2017): 2–12, https://doi.org/10.1016/j.medengphy.2017.06.045.

195. S. Morganti, M. Conti, M. Aiello, et al., "Simulation of Transcatheter Aortic Valve Implantation through Patient-Specific finite Element Analysis: Two Clinical Cases," *Journal of Biomechanics* 47 (2014): 2547–2555, https://doi.org/10.1016/j.jbiomech.2014.06.007.

196. R. P. Ghosh, G. Marom, M. Bianchi, D. Karl, W. Zietak, and D. Bluestein, "Numerical Evaluation of Transcatheter Aortic Valve Performance during Heart Beating and Its Post-Deployment fluid–structure Interaction Analysis," *Biomechanics and Modeling in Mechanobiology* 19, no. 5 (2020): 1725–1740, https://doi.org/10.1007/s10237-020-01304-9.

197. V. Govindarajan, C. Wanna, N. P. Johnson, et al., "Unraveling Aortic Hemodynamics Using Fluid Structure Interaction: Biomechanical Insights into Bicuspid Aortic Valve Dynamics With Multiple Aortic Lesions," *Biomechanics and Modeling in Mechanobiology* 24, no. 1 (2025): 17–27, https://doi.org/10.1007/s10237-024-01892-w.

198. K.-M. Bornemann and D. Obrist, "Leaflet Fluttering Changes Laminar–turbulent Transition Mechanisms past Bioprosthetic Aortic Valves," *Physics of Fluids* 37 (2025): 051911, https://doi.org/10.1063/5.0270405.

199. R. Eerdekens, V. Govindarajan, N. P. Johnson, et al., "Hemodynamic Response of Normal Aortic Valves to Stress Using Invasive, Non-Invasive, and Computational Techniques," *European Heart Journal—Imaging Methods and Practice* 3, no. 1 (2025): qyaf061, https://doi.org/10.1093/ehjimp/qyaf061.

200. M. Bianchi, G. Marom, R. P. Ghosh, et al., "Patient-Specific simulation of Transcatheter Aortic Valve Replacement: Impact of Deployment Options on Paravalvular Leakage," *Biomechanics and Modeling in Mechanobiology* 18, no. 2 (2019): 435–451, https://doi.org/10.1007/s10237-018-1094-8.

201. D. G. Owen, T. Schenkel, D. E. T. Shepherd, D. M. Espino, and D. G. Owen, "Assessment of Surface Roughness and Blood Rheology on Local Coronary Haemodynamics: a Multi-Scale computational Fluid Dynamics Study," *Journal of The Royal Society Interface* 17 (2020): 20200327, https://doi.org/10.1098/rsif.2020.0327.

202. M. Bonini, S. Sanjay, M. Balmus, et al., "Modeling the Hemodynamic Impact of Y-Incision Aortic Annular Enlargements on Aortic Valve Replacement and Valve-in-Valve Procedures," *Journal of Cardiovascular Translational Research* 18 (2025): 876–887, https://doi.org/10.1007/s12265-025-10634-x.

203. F. Nappi, L. Mazzocchi, C. Spadaccio, et al., "CoreValve vs. Sapien 3 Transcatheter Aortic Valve Replacement: a Finite Element Analysis Study." *Bioengineering* 2021, 52, 8 (5), https://doi.org/10.3390/bioengineering8050052.

204. M. C. B. Costa, S. D. F. Gonçalves, M. L. F. D. Silva, J. V. C. Fleury, R. Huebner, and A. H. D. F. Avelar, "The Influence of Leaflet Flutter of the Aortic Valve Bioprostheses on Leaflet Calcification and Endothelial Activation," *Computers in Biology and Medicine* 187 (2025): 109765, https://doi.org/10.1016/j.compbiomed.2025.109765.

205. E. L. Johnson, M. R. Rajanna, C.-H. Yang, and M.-C. Hsu, "Effects of Membrane and Flexural Stiffnesses on Aortic Valve Dynamics: Identifying the Mechanics of Leaflet Flutter in Thinner Biological Tissues," *Forces in Mechanics* 6 (2022): 100053, https://doi.org/10.1016/j.finmec.2021.100053.

206. A. H. Sofiyev, "A New Approach to Solution of Stability Problem of Heterogeneous Orthotropic Truncated Cones With Clamped Edges Within Shear Deformation Theory," *Composite Structures* 304, no. P2 (2023): 116411, https://doi.org/10.1016/j.compstruct.2022.116411.

207. A. Mirza, C.-P. D. Hsu, A. Rodriguez, et al., "Computational Model for Early-Stage Aortic Valve Calcification Shows Hemodynamic Biomarkers," *Bioengineering* 11, no. 10 (2024): 1–16.

208. P. Corso and D. Obrist, "On the Role of Aortic Valve Architecture for Physiological Hemodynamics and Valve Replacement, Part I: Flow Configuration and Vortex Dynamics," *Computers in Biology and Medicine* 176 (2024): 108526, https://doi.org/10.1016/j.compbiomed.2024.108526.

209. P. Corso and D. Obrist, "On the Role of Aortic Valve Architecture for Physiological Hemodynamics and Valve Replacement, Part II: Spectral Analysis and Anisotropy," *Computers in Biology and Medicine* 176 (2024): 108552, https://doi.org/10.1016/j.compbiomed.2024.108552.

210. L. Crugnola, C. Vergara, L. Fusini, et al., "Computational Hemodynamic Indices to Identify Transcatheter Aortic Valve Implantation

Degeneration," *Computer Methods and Programs in Biomedicine* 259 (2025): 108517, https://doi.org/10.1016/j.cmpb.2024.108517.

211. T. R. G. Cartlidge, M. K. Doris, S. L. Sellers, et al., "Detection and Prediction of Bioprosthetic Aortic Valve Degeneration," *Journal of the American College of Cardiology* 73, no. 10 (2019): 1107–1119, https://doi.org/10.1016/j.jacc.2018.12.056.

212. A. Zingaro, I. Burba, D. Oks, et al., "Advancing Aortic Stenosis Assessment: Validation of Fluid-Structure Interaction Models against 4D Flow MRI Data," *ArXiv* 2404 (2024): 08632, https://doi.org/10.48550/arXiv.2404.08632.

213. S. Morganti, N. Brambilla, A. S. Petronio, A. Reali, F. Bedogni, and F. Auricchio, "Prediction of Patient-Specific Post-Operative Outcomes of TAVI Procedure: the Impact of the Positioning Strategy on Valve Performance," *Journal of Biomechanics* 49, no. 12 (2016): 2513–2519, https://doi.org/10.1016/j.jbiomech.2015.10.048.

214. G. Athappan, R. Dilip Gajulapalli, P. Sengodan, et al., "Influence of Transcatheter Aortic Valve Replacement Strategy and Valve Design on Stroke after Transcatheter Aortic Valve Replacement," *Journal of the American College of Cardiology* 63, no. 20 (2014): 2101–2110, https://doi.org/10.1016/j.jacc.2014.02.540.

215. F. Sturla, M. Ronzoni, M. Vitali, et al., "Impact of Different Aortic Valve Calcification Patterns on the Outcome of Transcatheter Aortic Valve Implantation: a Finite Element Study," *Journal of Biomechanics* 49, no. 12 (2016): 2520–2530, https://doi.org/10.1016/j.jbiomech.2016.03.036.

216. N. W. Bressloff, "Leaflet Stresses during Full Device Simulation of Crimping to 6 Mm in Transcatheter Aortic Valve Implantation, TAVI," *Cardiovascular Engineering and Technology* 13, no. 5 (2022): 735–750, https://doi.org/10.1007/s13239-022-00614-6.

217. C. Martin and W. Sun, "Simulation of Long-Term Fatigue Damage in Bioprosthetic Heart Valves: Effects of Leaflet and Stent Elastic Properties," *Biomechanics and Modeling in Mechanobiology* (2014): 759–770, https://doi.org/10.1007/s10237-013-0532-x.

218. D. B. Smith, M. S. Sacks, P. M. Pattany, and R. Schroeder, "Fatigue-Induced Changes in Bioprosthetic Heart Valve Three-Dimensional Geometry and the Relation to Tissue Damage," *Journal of Heart Valve Disease* 8, no. 1 (1999): 25–33.

219. Y. Dabiri and K. Narine, "Roles of the Leaflet Geometry in the Structural Deterioration of Bioprosthetic Aortic Valves," *Prosthesis* 7 (2025): 86, https://doi.org/10.20944/preprints202505.0675.v1.

220. M. Marino, M. I. Converse, K. L. Monson, and P. Wriggers, "Molecular-Level Collagen Damage Explains Softening and Failure of Arterial Tissues: a Quantitative Interpretation of CHP Data With a Novel Elasto-Damage Model," *Journal of the Mechanical Behavior of Biomedical Materials* 97 (2019): 254–271, https://doi.org/10.1016/j.jmbbm.2019.04.022.

221. E. Peña, B. Calvo, M. A. Martìnez, and M. Doblaré, "An Anisotropic Visco-Hyperelastic Model for Ligaments at Finite Strains. Formulation and Computational Aspects," *International Journal of Solids and Structures* 44 (2007): 760–778, https://doi.org/10.1016/j.ijsolstr.2006.05.018.

222. S. H. Alavi, V. Ruiz, T. Krasieva, E. L. Botvinick, and A. Kheradvar, "Characterizing the Collagen Fiber Orientation in Pericardial Leaflets under Mechanical Loading Conditions," *Annals of Biomedical Engineering* 41, no. 3 (2013): 547–561, https://doi.org/10.1007/s10439-012-0696-z.

223. G. A. Holzapfel and R. W. Ogden, "A Damage Model for Collagen Fibres With an Application to Collagenous Soft Tissues," *Proceedings of the Royal Society A* 476 (2020): 20190821, https://doi.org/10.1098/rspa.2019.0821.

224. W. Zhang, S. Motiwale, M.-C. Hsu, and M. S. Sacks, "Simulating the Time Evolving Geometry, Mechanical Properties, and Fibrous Structure of Bioprosthetic Heart Valve Leaflets under Cyclic Loading," *Journal of the Mechanical Behavior of Biomedical Materials* 123 (2021): 104745, https://doi.org/10.1016/j.jmbbm.2021.104745.

225. M. Alloisio and T. Christian Gasser, "Fracture of Porcine Aorta—Part 2: FEM Modelling and Inverse Parameter Identification," *Acta Biomaterialia* 167 (2023): 158–170, https://doi.org/10.1016/j.actbio.2023.06.020.

226. O. Gültekin, H. Dal, and G. A. Holzapfel, "A Phase-Field approach to Model Fracture of Arterial Walls: Theory and Finite Element Analysis," *Computer Methods in Applied Mechanics and Engineering* 312 (2016): 542–566, https://doi.org/10.1016/j.cma.2016.04.007.

227. D. Balzani, J. Schröder, and D. Gross, "Simulation of Discontinuous Damage Incorporating Residual Stresses in Circumferentially Overstretched Atherosclerotic Arteries," *Acta Biomaterialia* 2 (2006): 609–618, https://doi.org/10.1016/j.actbio.2006.06.005.

228. E. Peña, B. Calvo, M. A. Martínez, and M. Doblaré, "On Finite-Strain Damage of Viscoelastic-Fibred Materials Application to Soft Biological Tissues," *Int J Numer Meth Engng* 74 (2008): 1198–1218, https://doi.org/10.1002/nme.2212.

229. E. Maher, A. Creane, C. Lally, and D. J. Kelly, "An Anisotropic Inelastic Constitutive Model to Describe Stress Softening and Permanent Deformation in Arterial Tissue," *Journal of the Mechanical Behavior of Biomedical Materials* 12 (2012): 9–19, https://doi.org/10.1016/j.jmbbm.2012.03.001.

230. K. Linka, M. Hillgärtner, and M. Itskov, "Fatigue of Soft Fibrous Tissues: Multi-Scale Mechanics and Constitutive Modeling," *Acta Biomaterialia* 71 (2018): 398–410, https://doi.org/10.1016/j.actbio.2018.03.010.

231. C. Martin and W. Sun, "Modeling of Long-Term Fatigue Damage of Soft Tissue With Stress Softening and Permanent Set Effects," *Biomechanics and Modeling in Mechanobiology* 12 (2013): 645–655, https://doi.org/10.1007/s10237-012-0431-6.

232. J. Lopez, Z. Li, and G. Oger, "An LBM-FEM Robust and Efficient Fluid–structure Coupling Scheme for Partitioned Numerical Simulation of Blood Flow-Aortic valve Interaction," *Computers in Biology and Medicine* 196 (2025): 110578, https://doi.org/10.1016/j.compbiomed.2025.110578.

233. F. Ballarin and G. Rozza, "POD–Galerkin Monolithic Reduced Order Models for Parametrized Fluid-Structure Interaction Problems," *International Journal for Numerical Methods in Fluids* 82 (2016): 1010–1034, https://doi.org/10.1002/fld.

234. J. Franz, K. Czechowicz, I. Waechter-Stehle, et al., "An Orifice Shape-Based Reduced Order Model of Patient-Specific Mitral Valve Regurgitation," *Engineering Applications of Computational Fluid Mechanics* 15, no. 1 (2021): 1868–1884, https://doi.org/10.1080/19942060.2021.1995048.

235. I. Fumagalli, L. Dede, A. Quarteroni, and L. Dede, "A Reduced 3D - 0D Fluid—Structure Interaction Model of the Aortic Valve That Includes Leaflet Curvature," *Biomechanics and Modeling in Mechanobiology* (2025): 2014, https://doi.org/10.1007/s10237-025-01960-9.

236. R. A. Gray and P. Pathmanathan, "Patient-Specific Cardiovascular Computational Modeling: Diversity of Personalization and Challenges," *Journal of Cardiovascular Translational Research* 11 (2018): 80–88, https://doi.org/10.1007/s12265-018-9792-2.

237. W. Mao, Q. Wang, S. Kodali, and W. Sun, "Numerical Parametric Study of Paravalvular Leak Following a Transcatheter Aortic Valve Deployment into a Patient-Specific Aortic Root," *Journal of Biomechanical Engineering* 140 (2018): 1–11, https://doi.org/10.1115/1.4040457.

238. A. Rassoli, X. Zhao, and Y. Yang, "Pericardia Are Still the Most Select Sources to Manufacture Percutaneous Heart Valves," in *Cardiovascular Explants*, ed. Ze Zhang, R Guidoin, and Lu Wang, (Springer, 2025), 485–532, https://doi.org/10.1007/978-3-031-85504-7_11.

239. B. B. Roe and D. Moore, "Design and Fabrication of Prosthetic Valves," *Experimental Medicine and Surgery* 16, no. 2 (1958): 177–182.

240. I. George, D. P. Rao, A. Jain, et al., "1-Year Results from a Multicenter Trial of a Polymer Surgical Mitral Valve," *JACC* 86 (2025): 515–526, https://doi.org/10.1016/j.jacc.2025.06.017.

241. M. A. Rezvova, K. Y. Klyshnikov, and A. A. Gritskevich, "Polymeric Heart Valves Will Displace Mechanical and Tissue Heart Valves: a New Era for the Medical Devices," *International Journal of Molecular Sciences* 24 (2023): 3963, https://doi.org/10.3390/ijms24043963.

242. Y. Wang, Y. Fu, Q. Wang, D. Kong, Z. Wang, and J. Liu, "Recent Advancements in Polymeric Heart Valves: from Basic Research to Clinical Trials," *Materials Today Bio* 28 (2024): 101194, https://doi.org/10.1016/j.mtbio.2024.101194.

243. M. Crago, A. L. A. B, S. F. A, et al., "The Evolution of Polyurethane Heart Valve Replacements: How Chemistry Translates to the Clinic," *Materials Today Communications* 33 (2022): 104916, https://doi.org/10.1016/j.mtcomm.2022.104916.

244. S. F. Melo, A. Nondonfaz, A. Aqil, et al., "Design, Manufacturing and Testing of a Green Non-Isocyanate polyurethane Prosthetic Heart Valve," *Biomaterials Science* 12 (2024): 2149–2164, https://doi.org/10.1039/d3bm01911j.

245. M. Sharabi, "Structural Motifs in Soft Fibrous Tissues Revealing Structure-Mechanics Relationships in Deformation and Tear Resistance for Biomimetic Material Design.Pdf," *Advanced Healthcare Materials* (2025): 2500153, https://doi.org/10.1002/adhm.202500153.

246. M. J. Vernon, A. R. Ihdayhid, P. Mela, et al., "3D Printing of Heart Valves," *Trends in Biotechnology* 42, no. 5 (2024): 612–630, https://doi.org/10.1016/j.tibtech.2023.11.001.

247. P. Chansoria, J. Blackwell, E. L. Etter, et al., "Rationally Designed Anisotropic and Auxetic Hydrogel Patches for Adaptation to Dynamic Organs," *Advanced Functional Materials* 15 (2022): 2207590, https://doi.org/10.1002/adfm.202207590.

248. S. Domaschke, G. Fortunato, and A. E. Ehret, "Random Auxetics from Buckling Fi Bre Networks," *Nature Communications* 10, no. 4863 (2019): 1–8, https://doi.org/10.1038/s41467-019-12757-7.

249. V. Gupta and A. Chanda, "Expansion Potential of Novel Skin Grafts Simulants With I-Shaped Auxetic Incisions," *Biomedical Engineering Advances* 5 (2023): 100071, https://doi.org/10.1016/j.bea.2023.100071.

250. Y. Jin, C. Xie, Q. Gao, et al., "Fabrication of Multi-Scale and Tunable Auxetic Scaffolds for Tissue Engineering," *Materials & Design* 197 (2021): 109277, https://doi.org/10.1016/j.matdes.2020.109277.

251. R. L. Li, J. Russ, C. Paschalides, et al., "Mechanical Considerations for Polymeric Heart Valve Development: Biomechanics, Materials, Design and Manufacturing," *Biomaterials* 225 (2019): 119493, https://doi.org/10.1016/j.biomaterials.2019.119493.

252. L. D. Bianco, N. M. Pugno, and B. Schmuck, "Artificial Spider Silk Fibers With Embedded Magnetite Nanoparticles," *Macromolecular Materials and Engineering* 310, no. 11 (2025): 00249, https://doi.org/10.1002/mame.202500249.

253. S. Goutianos and T. Peijs, "On the Low Reinforcing Efficiency of Carbon Nanotubes in High-Performance polymer Fibres," *Nanocomposites* 7, no. 1 (2021): 53–69, https://doi.org/10.1080/20550324.2021.1917815.

254. G. Greco, B. Schmuck, L. Del Bianco, et al., "High-Performance Magnetic Artificial Silk Fibers Produced by a Scalable and Eco-Friendly Production Method," *Advanced Composites and Hybrid Materials* 7, no. 163 (2024), https://doi.org/10.1007/s42114-024-00962-y.

255. I. Kaur, L.-J. Ellis, I. Romer, et al., "Dispersion of Nanomaterials in Aqueous Media: towards Protocol Optimization," *Journal of Visualized Experiments* 2017, no. 130 (2017), https://doi.org/10.3791/56074.

256. I. A. Kinloch, J. Suhr, J. Lou, R. J. Young, and P. M. Ajayan, "Composites With Carbon Nanotubes and Graphene: an Outlook," *Science* 362 (2018): 547–553, https://doi.org/10.1126/science.aat7439.

257. M. Y. Emmert, B. A. Schmitt, S. Loerakker, et al., "Computational Modeling Guides Tissue-Engineered Heart Valve Design for Long-Term in Vivo Performance in a Translational Sheep Model," *Science Translational Medicine* 10 (2018): aan4587, https://doi.org/10.1126/scitranslmed.aan4587.

258. G. K. Jalandhra, L. Srethbhakdi, J. Davies, et al., "Materials Advances in Devices for Heart Disease Interventions," *Advanced Materials* 37 (2025): 2420114, https://doi.org/10.1002/adma.202420114.